Synthesis and Characterization of Zeolite A Using Bagasse Ash, as Bio-Silica Source for Water Hardness Removal

By: Mengistu Tadesse Mosisa

Thesis submitted to the Applied Chemistry Department, in Fulfillment of the Requirements for the Degree of Master of Science in Chemistry (Industrial Chemistry).

School of Applied Natural Science

Office of Graduate Studies

Adama Science and Technology University (ASTU)

Adama, Ethiopia

September, 2018

Synthesis and Characterization of Zeolite A Using Bagasse Ash, as Bio-Silica Source for Water Hardness Removal

By: Mengistu Tadesse Mosisa

Advisors**:** Dr. Eshetu Bekele

Dr. Eniyew Amare

Thesis submitted to the Applied Chemistry Department, in Fulfillment of the Requirements for the Degree of Master of Science in Chemistry (Industrial Chemistry).

School of Applied Natural Science

Office of Graduate Studies

Adama Science and Technology University (ASTU)

Adama, Ethiopia

September, 2018

Advisors Approval sheet

To: Applied Chemistry Department

Subject: Thesis Submission

This is to certify that the M.Sc thesis entitled "**Synthesis and Characterization of Zeolite A Using Bagasse Ash as Bio-Silica Source for Water Hardness Removal**". Submitted in partial fulfillment of the requirements for the degree of Masters in Industrial chemistry, the Graduate program of the department of applied chemistry, and has been carried out by Mengistu Tadesse Id. No GSR/0182/09, under our supervision. Therefore, we recommend that the student has fulfilled the requirements and hence hereby he can submit the thesis to the department.

---	---	---
Advisor	signature	Date
---	---	---
Advisor	signature	Date

Approval sheet

School of Applied Natural Sciences

Adama Science and Technology University

This is to certify that the thesis prepared by Mengistu Tadesse Mosisa Entitled: "**Synthesis and Characterization of zeolite A Using Bagasse Ash, as Bio-Silica Source for Water Hardness Removal**" and submitted in partial fulfillments of the requirements for the Degree of Masters of Science In Industrial Chemistry complies with the regulations of and meets the accepted standards with respect to originality and quality.

Signed by the Examining committee:

Chairman _____Signature _____ Date_____

Ex. Examiner _____Signature _____ Date_____

In. Examiner _____Signature _____ Date_____

Advisor _____ Signature _____ Date_____

Advisor _____ Signature _____ Date_____

DECLARATION

I, Mengistu Tadesse, author of the thesis '**Synthesis and Characterization of zeolite A using Bagasse Ash**, **as Bio-Silica source for water hardness removal**" hereby declare that all information in this document has been obtained and presented in accordance with academic rules and ethical conduct. I also declare that, as required by these rules and conduct, I have fully cited and referenced all material and results that are not original to this work.

Name: Mengistu Tadesse Mosisa

Signature:----------

Certified by:

Advisors: Dr Eshetu Bekele

Signature:_____

Dr Enyew Amare

Signature:----------

ACKNOWLEDGEMENTS

I would like to express my gratitude to my advisers Dr. Eshetu Bekele and Dr. Enyew Amare for their support, guidance and criticisms. I would like to thank the Technical Staff of Chemical Engineering program and my colleagues at Material Science and Engineering program, Demeke and Dr Dinsefa for their support and motivation. It was a pleasure working and interacting with them and to Andualem Marga and Bundi Roba for their immense help. Lastly, I would like to express my love to my family for their prayers, support, guidance, encouragement and patience.

Mengistu Tadesse Mosisa

September, 2018

List of Abbreviations and Acronyms

AAS	Atomic Absorption
CEC	Cation Exchange Capacity
DTG	Differential Thermal Gravimetric Analysis
HBA	Hydrochloric Acid Treated Bagasse Ash
LTA	Linde Type A
PBU	Primary Building
RBA	Raw Bagasse Ash
SBU	Secondary Building Unit
SEM	Scanning Electron Microscopy
TGA	Thermal Gravimetric Analysis
WHO	World Health Organization
XRD	X-Ray Diffraction

Table of Contents

Contents Page

List of Tables

List of figures

ABSTRACT

Zeolite A is a synthetic sodium alumino-silicate which is important synthetic zeolites widely used for separation and adsorption in industry. However, its wide application has been constrained by availability and cost of raw materials specifically the silica sources. Therefore, in this study low cost industrial byproduct Bagasse Ash was used as a Bio-Silica and synthesis of zeolite A for application of water hardness removal. Na_2CO_3 *and* Al_2O_3 *were used to replace the expensive* $NaAlO_2$ *on Ethiopian market to adjust molar ratio of bagasse ash as required for zeolite A. The process parameters for the synthesis of zeolite A for water hardness removal, such as the effect of ageing time (gel formation), crystallization time and crystallization temperature were systematically studied to optimize the control variables. The composition, morphology, crystalline phase, Thermal stability and CEC of synthesized zeolite A was further characterized using Chemical Method, SEM, XRD, DTA and AAS. Finally, the performance of the synthesized zeolite A in the removal of* Ca^{2+} *and* Mg^{2+}*, highly water hardness causing metal ions, was investigated. The result showed that phase-pure zeolite A can be synthesized from Bagasse Ash at reactant molar ratio, of* $1.3Na_2O: 0.6Al_2O_3 :1SiO_2: xH_2O$*, at 110°C reaction temperature, reaction time of 3h, and aging time of 3h and the synthesized zeolite efficiently removed 96.43%* Ca^{2+} *and 99.44%* Mg^{2+} *ions from synthetic very hard water. The removal of* Ca^{2+}*and* Mg^{2+} *from water which occurred through precipitation and ion exchange mechanisms was seen to be more efficient comparing to the previous studies. The adsorption of* Ca^{2+} *and* Mg^{2+} *ions by the synthesized zeolite A follows Langmuir adsorption isotherm with 555.54ml/g/g and 65.78ml/g/g maximum Sorption Capacity respectively and pseudo-second- order kinetic model. In conclusion, Bagasse Ash could be one of the alternative source of Bio-Silica extraction for different purpose and the synthesized zeolite Na-A showed an excellent potential to removal of water hardness.*

Keyword*s Bagasse Ash, zeolite A, Ageing, Crystallization, Characterization and Water hardness*

.

1. Introduction

1.1. Background of the study

Zeolites are three dimensional crystalline, hydrated aluminosilicate materials, which have enormous scientific and industrial significance. It has widely applicable for purification, drying, environmental treatment, and water softener in detergent industry, radioactive waste storage, and treatment of liquid waste. Moreover, as a used solid catalyst for cracking of hydrocarbons, catalytic reforming, hydroisomerization, dewaxing of hydrocarbon oils, isoparaffin/olefin alkylation, transalkylation of aromatics, and methanol to gasoline conversion (Lijalem *et al*., 2015). These applications are based on their inherent properties such as uniform pore size and shape; acidic properties, mobile extra framework cation and surface properties like hydrophilicity and hydrophobicity (Upenyu *et al*., 2017).

Out of the various low silica zeolites, zeolite A is one of the microporous crystalline aluminosilicate zeolites which have a channel opening size of 4.2 nm (Hu *et al*., 2017). The small pore size of zeolite A makes the separation of small molecules by difference in size possible. Zeolite A has a pore opening of 4A, which can be modified to 5A or 3A by ion exchange with aqueous solutions of calcium or potassium salts, as a result of their adsorption, ion exchange and porosity properties, zeolite A crystals are widely applied in various applications such as household products, Ion Exchanger, aquaculture and petrochemical-related industry (Xu *et al*., 2013).

Zeolite A, LTA (Linde Type A) or 4A is a synthetic sodium aluminosilicate represented by the formula: $Na_{12}[(AlO2)_{12}(SiO2)_{12}].27H_2O$. The crystal structure is cubic with a lattice parameter of 12.32 Å (Gustavo *et al*., 2015). It has a high cation exchange capacity as each alumina tetrahedral in the framework introduces a negative charge that must be compensated by a cation. This property gave to zeolite A a water softening abilities by ion exchanging Ca^{2+} and to a lesser extent Mg^{2+} for Na+ with the value ranging from 510 meqCa2+/100 g of anhydrous solid to 592 meq$Ca^{2+/}$100 g at 294.1 K and 1000 ppm (Garcia *et al*., 2015) thereby preventing precipitation of calcium compounds.

The hardness of water has less health effect, but it has a great economic problems both at domestic and industrial levels; for example domestically it cause wastage of soap during washing and formation of scales on cooking material and also since it increases the boiling point of water it results consumption of energy and fuel. At industrial level it is causing high economic effect on industries (Li *et al*., 2012).

Traditionally, water purification plants were used lime and soda ash for the removal of water hardness. One of the main drawbacks of this process is the generation of large amounts of liquid sludge as well as the need for recarbonation of the treated water (Dimirkou and Doula, 2008). The use of polyphosphates in removing water hardness is also practiced but results in massive discharge of phosphates in water bodies which lead to eutrophication (Xue *et al*., 2014). Various other methods including membrane precipitation, phytoextraction, flocculation, solvent extraction, ultrafiltration, reverse osmosis, electrodialysis, and adsorption have been studied for the removal of a wide variety of cations from water streams including magnesium and calcium (Seifi *et al*., 2011). Most of these are either inefficient or expensive and result in the generation of large amounts of sludge (Upenyu *et al*., 2017). Activated carbon is considered to be a particularly competitive and effective process for the removal of cations but it has been hampered by the high costs associated with production and regeneration of spent carbon. Therefore, the use of low-cost ion exchangers such as zeolites is an attractive method for the removal of metals from aqueous solutions.

The use of Zeolites in the removal of water hardness in domestic water mainly associated with their unique porous properties (Lijalem *et al*., 2015). For the synthesis of Zeolite A, mostly pure chemical grade reagents are used with the expectation that fulfill all the aforementioned requirements (Hu *et al*., 2017). However, concerns related to high energy consumption, carbon economy and high production costs have called the attention of researchers to seek cheaper raw materials for zeolite synthesis (Li *et al*., 2012). So far a number of studies have been conducted on the synthesis of zeolite A from raw materials such as kaolin, diatomite, bentonite, fly ash, or smectite (Alves *et al*., 2017). For instance,

Kaolin has been widely investigated for the synthesis of zeolites as it possesses the appropriate SiO_2/Al_2O_3 ratio and the effect of different factors that affecting the synthesis process was extensively reported (Garcia *et al*., 2015). However, kaolin must be activated in the form of metakaolin by calcination at high temperature ranging from 773 to 1273 K in order to produce an amorphous material that can be easily digested during zeolite synthesis that shows the high energy consumption of zeolite A synthesis from kaolin (Lijalem *et al*., 2015). Moreover, the high iron content encountered when using kaolin for zeolite production might need various techniques for removal of iron and these separation procedures represent additional costs to the general process (Loiola *et al*., 2010 and Li *et al*., 2012)..

These demand finding alternative materials such as industrial byproducts as raw materials for the synthesis of zeolite A for its wide uses for human health related application such as water softening and medical applications.

Many researchers have been involved in synthesizing different types of zeolites from industrial solid waste. As mentioned in Thuadaij and Mukda, (2016) zeolite A derived from Buriram sugarcane bagasse ash with high CEC value 351meq/100g for water hardness removal. Moreover, Norsuraya *et al*., (2016) have studied that zeolites su*ch* as Na-X, Na-A, Na-p and hydroxy-sodalite are the favorable zeolite types that can be prepared from silica bearing solid waste, such as Bagasse Ash, Rice husk Ash, Sugarcane leaf Ash, Rice straw Ash, Wheat Straw Ash, Corn Cob Ash and Sugarcane Bagasse fly Ash. In fact, to produce a single crystal of zeolite from the wastes was still a challenging task, even though the two step method was already applied. In the previous attempts, prepared zeolite X crystal was accompanied with zeolite A, P1, or sodalite, while synthesized zeolite A was contaminated with hydroxy-sodalite or amorphous aluminosilicate (Loilo *et al*., 2012). Among the three common types, zeolite X is the most porous but the most difficult to be prepared in high purity. This could be due to the thermodynamically metastable characteristic of highly porous Faujasite (Chang *et al*., 2000). Sodalite formation during zeolitization may not be preferred due to its low cation exchange capacity and small accessible pore size (2.3 Å) (Querol *et al*.,2002). For obtaining the pure phase, after preparing a suitable silica–alumina source, the

crystallization conditions during hydrothermal method including the molar ratios of the components in the reaction mixture should be carefully controlled.

From industrial solid wastes up to present, most literatures used coal fly ash (CFA) as a low cost silica–alumina source for synthesizing these materials. However, the alkali extract from CFA contains not only silicon and aluminum which are the main building blocks of zeolites, but also several other compounds are dissolved during the process. Naturally, biomass ashes including Bagasse Ash contain less chemical components than CFA, thus extraction of these materials produces supernatant with lower unrelated component concentration other than silica and alumina. Even though, the possible harmful traces such as Mo, As, Cr, Pb and V inside the CFA supernatant are likely to be incorporated in the zeolite structure during synthesis (Santasnachok *et al*., 2015), but the contamination possibility is hard to be completely eliminated, Bagasse Ash is relatively a purer precursor that can be preferred to ensure the quality and reproducibility of the end products using the predetermined zeolitization conditions than other solid wastes (Sepehr *et al*., 2013).

1.2. Statement of the problems

From the Starting date of their discovery, various applications of zeolites have been noted in almost all industries. However, the main problem in the wide application of zeolite is the availability and cost of raw material specifically the silica source for its synthesis. The preparation of synthetic zeolites from silica and alumina chemical sources is expensive. Hence, cheaper raw materials, such as Industrial by products, clay minerals, natural zeolites, coal ashes, municipal solid waste incineration ashes and industrial slag, have been utilized as starting materials for zeolite synthesis. Related to the use of waste materials in zeolite synthesis for its application of water purification is the concern of this study.

Reports indicated that problems related to water hardness in Ethiopia is diverse. For instance high value was recorded in spring water samples from Oromiya (1100 mg/L); tap water from Addis Ababa (1600 mg/L), and well water samples from the Afar region (12,800 mg/L). Forty-two of spring water, twenty-five of tap water and eighty-seven of

the well water samples were exceeded the national recommended limit for total water hardness (ES 2001). Moreover, removal of water hardness is heavily depending on imported materials. On the other hand Sugar Industries generated huge quantities of Bagasse Ash as a byproduct and causing environmental problems. Consequently, the advance of new procedures for the recycling of this waste which is quartz abundant as silica source in the synthesis of Zeolite from bagasse Ash has a dual benefit such as to minimize environmental burden and substitute imported zeolites for its application of water hardness removal. Therefore, this study aimed at synthesis of zeolite A from Bagasse Ash as Bio-Silica sources with an adapted pre-treatment procedure for water hardness removal.

1.3. Objectives of the study

1.3.1. General objective

The major objective of this study is to Synthesis zeolite A using Bagasse Ash as a Bio-Silica source and to investigate the practical application of the synthesized zeolite A in water hardness removal.

1.3.2. Specific objectives

The specific objectives of this study are:

- To synthesis zeolite A using bagasse Ash as Bio-Silica source and inorganic reagent as additional source of Al_2O_3 and Na_2O (to adjust the molar ratio).
- To characterize the synthesized zeolite A
- To investigate the water hardness removal capacity of synthesized zeolite A
- To study the mechanism of the adsorption isotherm and kinetic models

1.4. Significance of the study

The importance of zeolites in various industries cannot be understated. The work proposed in this study is the first of its kind in the country. Although work has been carried out on the use of zeolites in removing water hardness, treating municipal and industrial waste waters, little is known on the efficacy of synthesized zeolites on water hardness removal. The results will benefit the industrial sector as most of the imported resin used for water hardness removal will be substituted by synthesized zeolite A from BA. Also, it would be a viable alternative to Biosilica for various purposes in Ethiopia.

1.5. The scopes of the Study

In order to reach this objective, the scope of the present work was limited the following activities, to synthesis, characterize Na-A zeolite from Bagasse Ash for water hardness removal.

2. Review of Literatures

2.1. General Overview of Zeolite

Zeolites are crystalline, hydrated aluminosilicates of alkaline or alkaline earth metals. The frameworks are composed of $[SiO_4]^{4-}$ and $[A1O_4]^{5-}$ tetrahedra, which corner-share to form different open structures. The tetrahedra are linked together to form cages connected by pore openings of defined size; depending on the structural type, the pore sizes range from approximately 0.3-1 nm (Hu *et al.*, 2017). The negative charge on the lattice is neutralized by the positive charge of cations located within the material's pores. In the basic zeolites, these are usually univalent and bivalent metals or a combination. The metal cations may be replaced by acidic protons via ion-exchange to ammonium and subsequent calcination. By reason of electrostatic forces it is not possible to make an Al-O-Al bond. They are made up of "T-atoms" which are tetrahedrally bonded to each other with oxygen bridges. Other "T-atoms" such as P, Ga, Ce, B and Be can also exist in the framework. Due to their exceptional properties, zeolites have been widely used in numerous technical applications as catalysts, adsorbents and ion exchangers (Sean and Yoshio, 2009).

The structure formula of zeolite is based on the crystallographic unit cell: $Mx/n\ [(AlO_2)x(SiO_2)y]\ wH_2O$, where (M) is an alkali or alkaline earth cation, (n) is the valence of the cation, (w) is the number of water molecules per unit cell, x and y are the total number of tetrahedra per unit cell, and the ratio y/x usually has values of 1 to 5, though for the silica zeolite, y/x can be raging from 10 to 100 (Upenyu *et al*., 2017).

Zeolites have been well studied in terms of the relations among structure, properties and synthesis. Nowadays 180 synthetic zeolites are known. Some of the earlier synthetic zeolites include zeolites A, X, Y, L, ZSM-5 and omega. The Atlas of Zeolite Structure Types published and frequently updated by the IZA Structure Commission, assigns a three - letter code to be used for a known framework topology irrespective of composition. Illustrative codes are LTA for Linde zeolite A, FAU for molecular sieves with a Faujasite topology (e.g., zeolites X, Y), MOR for the mordenite topology and MFI for the ZSM - 5 and silicalite topologies and AFI for the aluminophosphate AlPO4-5

topology. The acceptance of a newly determined structure of a zeolite or molecular sieve for inclusion in the official Atlas is reviewed and must be approved by the IZA Structure Commission. The IZA Structure Commission was given authority at the Seventh International Zeolite Conference (Tokyo, 1986) to approve and/or assign the three - letter structure code for new framework topologies (Meier and Olson, 1987).

A typical crystal chemical formula for zeolite A (LTA) would be:

$$| Na_{12} (H_2O)_{27} | [Al_{12} Si_{12} O_{48}] .$$

Here, the fact that the host is 3-dimensional and can be constructed by linking double 4-rings as composite building units is highlighted. The description of the pores indicates that there are sodalite cages and a 3-dimensional channel system which contains α-cavities (Figure 2.1, Hagen, 1999).

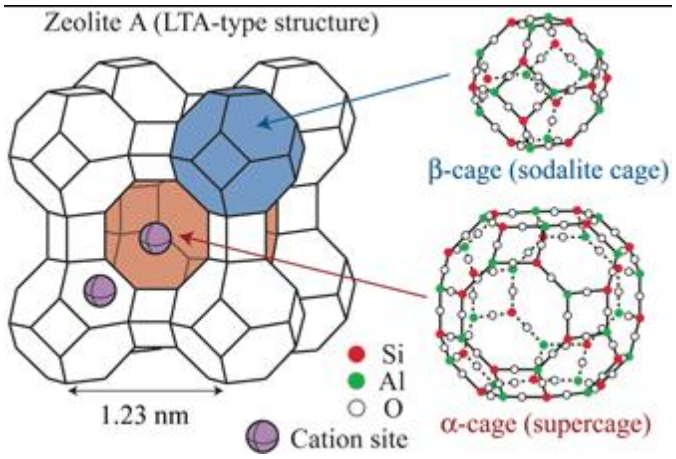

Figure: 2.1. Features of the pores in zeolite A (IZA code LTA): the sodalite cage, the a-cavity the 3-dimensional channel system, and the 8-ring defining the 0.41nm effective channel width.

In most zeolite structures the primary structural units, the AlO_4 or SiO_4 tetrahedra, are assembled into secondary building units which may be simple polyhedra, such as cubes, hexagonal prisms or cubo-octahedra. The final framework structure consists of assemblages of the secondary units. More than 70 novel, distinct framework structures of

zeolites are known. They exhibit pore sizes from 0.3 to 1.0 nm and pore volumes from about 0.10 to 0.35 cm^3.

2.2. Characteristics of zeolite

Porous materials are classified by their pore size into microporous and mesoporous materials. Microporous materials have pore diameters of less than 2 nm. Microporous materials are often used in laboratory environments to facilitate contaminant-free exchange of gases. Mold spores, bacteria, and other airborne contaminants will become trapped, while allowing gases to pass through the material. This allows for a sterile environment in the contained area. Zeolites are a very important member of this family (Xu *et al*., 2007).

Mesoporous materials are those with pores in the range 20-500Å in diameter. They have huge surface areas, providing a vast number of sites where sorption processes can occur. These materials have numerous applications in catalysis, separation and many other fields. The synthesis of these materials is of considerable interest and is constantly being developed to introduce different properties (Hoets, 2001).Typical mesoporous materials include some kinds of silica and alumina that have similar sized fine mesopores. Mesoporous oxides of niobium, tantalum, titanium, zirconium, cerium and tin have also been reported.

2.3. Structures of zeolite

Zeolites have interesting properties due to their anionic framework and exchangeable cations. Zeolite refers to a crystalline aluminosilicate with a corner sharing TO_4 (T = Si or Al) tetrahedra forming a three dimensional four- connected framework with uniformly sized pores of molecular dimensions.

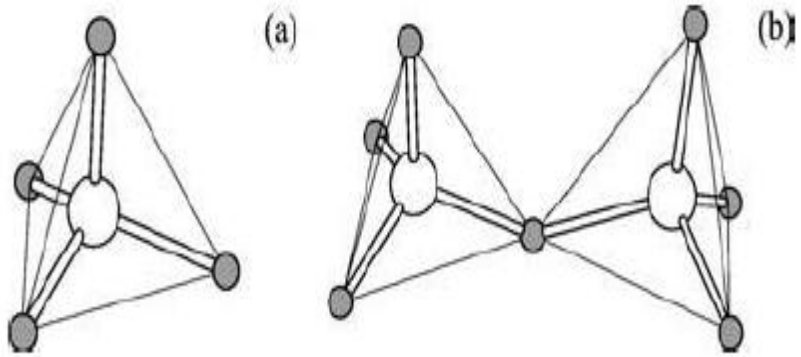

Figure 2.2: (a) TO4 tetrahedron. (b) Tetrahedra sharing a common oxygen vertex (Xu *et al*., 2007).

As indicated in Figure 2.2, the primary building unit of the zeolite structure has a central atom, silicon or aluminium with four oxygen atoms at the corners. A tetrahedron is formed with an oxygen atom being shared by two tetrahedra. Zeolites constructed from SiO4 and AlO4 tetrahedra possess an anionic framework, the negative charge of which is compensated by extra framework cations. Cations in the channels can be exchanged easily hence the term exchange or extra framework cations. Si and Al are not exchanged under ordinary conditions. They are called framework cations (Top, 2001). Exchangeable cations include lithium, cadmium, lead, zinc, copper, ammonium, silver and protons (Kwakye- Awuah, 2008). Zeolites have a uniform pore structure determined by the crystal structure with known pore diameter channels between 3 and 10 Å. The channels may be circular or elliptical, tubular or containing periodic cavities and straight or zigzag. A ring of oxygen atoms define the aperture of each channel the pore size. There may be 4, 5, 6, 8, 10 or 12 oxygen atoms in a ring. Pore size and structure of a zeolite affect the selectivity of a reaction (Hagen, 1999).

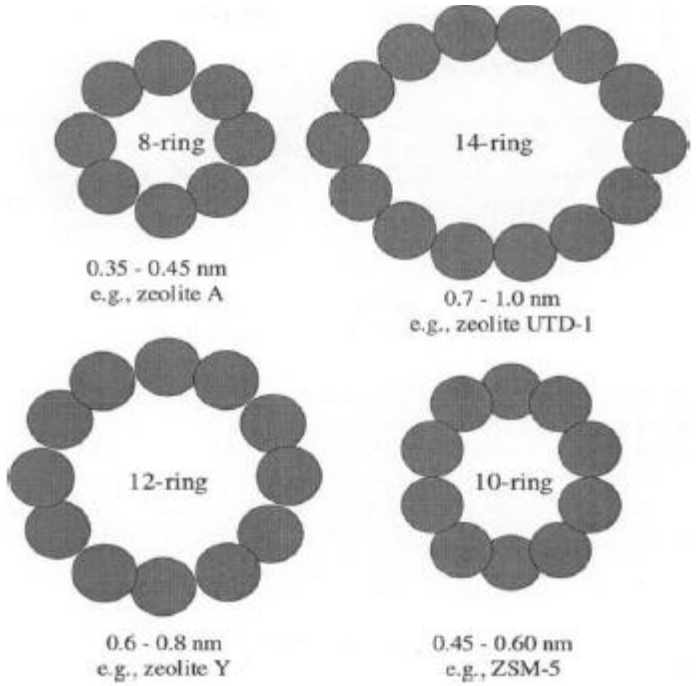

Figure 2.3: Illustration of zeolite pore sizes with oxygen atoms **(**Xu *et al***.,** 2007).

2.4. Applications of Zeolite

Zeolite has a wide range of applications. Currently, the use of zeolites is recognised and used in many industries. The largest is its use in the making of detergents. Others include:

2.4.1. Gas Purification and Separation

Zeolites act as molecular sieves. They are used to purify or sweeten natural gases through the removal of impurities such as carbon dioxide, sulphur dioxide and water. In addition to upgrading natural gas, zeolites are used to separate oxygen and nitrogen in pressure swing adsorption columns (Lijalem *et al*., 2015).

2.4.2. Ion exchange

The enclosed cavities contain both the metal cations and water molecules. The cations are loosely bound to the lattice and thus engage in ion exchange. The water molecules can

also be reversibly driven off in most zeolites. Cation exchange of zeolites is used routinely in modifying the properties of zeolite products used in adsorption and catalysis. The largest ion exchange application of zeolites is in its use as a builder for detergents (Upenyu *et al*., 2017).

2.4.3. Catalysis

Applications of zeolites include its use to catalyze the conversion of crude oil to more useful products such as gasoline, kerosene and other smaller hydrocarbons. Reactions involved include hydro cracking, hydro-isomerization, aromatization and dehydrogenation of cyclohexanes. Advantage of using zeolite is that these catalysts because of their specific pores and cages not all products can be formed resulting in selectivity of the reaction i.e. fraction of desired products of all products that are formed. Zeolites are extremely useful as catalysts for several important reactions involving organic molecules (Szostak, 2001). The most important are cracking, isomerization and hydrocarbon synthesis. Zeolites are able to promote a diverse range of catalytic reactions including acid-base and metal induced reactions; serve as acid catalysts and can be used to support active metals or reagents (Barthomeuf, 1996). Zeolites can be shape-selective catalysts either by transition state selectivity or by exclusion of competing reactants on the basis of molecular diameter (Sobolev *et al*., 1993). They have also been used as oxidation catalysts. The reactions can take place within the pores of the zeolite, which allows a greater degree of product control (Szostak, 2001).

2.4.4. Light weight Construction Materials

Natural zeolite can be used to prepare lightweight concrete for construction. Its porous silicate structure makes it much lighter than sand with an increased volume per ton but with similar hardness and strength. Zeolite is free from clay which reduces the overall strength of concrete and its porous structure holds moisture which facilitates a more rapid curing of concrete. When added to Portland cement as a Pozzolan, it can reduce chloride permeability and improve workability. It reduces weight and helps moderate water content while allowing for slower drying which improves break strength (Tubana *et al*., 2012).

2.4.5. Waste Water Treatment Media

Zeolites contribute to a cleaner, safer environment in a great number of ways. In fact nearly every application of zeolites has been driven by environmental concerns or plays a significant role in reducing toxic waste. As zeolites are a granular material, solid and suspended particles are trapped between the grains. The porous structure also causes colloid particles from both organic and mineral origin to be removed from the water (Szostak, 2001; Thompson, 1998). The capacity for the removal of solid particles is up to 45% greater than the capacity of sand with an equivalent particle size distribution. Certain natural zeolites have a high affinity for ammonium ions and are being used in a tertiary water treatment system.

2.4.6. Radioactive Waste Treatment

Natural zeolite has a high ion exchange capacity and a particular affinity for heavy metal cations. It can absorb elements such as strontium 90, caesium 137 and other radioactive isotopes from solutions and hold them in its 3 dimensional crystal framework. Zeolites react readily with cement and glass systems thus allowing the radioactive waste to be entrapped and contained safely. Zeolites are physically robust and resistant to nuclear degradation, and they are less expensive than organic ion exchange resins (Abd El Hay *et al*., 2016).

2.4.7. Pool Filtration Media

Zeolites offer superior performance for sand and carbon filters, giving purer water and higher output rates with less maintenance required. The highly porous structure of zeolites captures particulate contamination down to 4 microns in size. Chemicals such as chlorine, algaecides and flocculants can change the pH of pool water. In addition, environmental factors as well as the quality of the fill water can create changes in the pH of a swimming pool (Dyer and White, 1999). The use of zeolites results in lower chlorine consumption and a better swimming environment in pools. Zeolites also adsorb ammonia and its compounds thus reducing and preventing their formation (Dyer and White, 1999) as cited by Kwakye-Awuah (2008).

2.4.8. Fertilizer and Feed Additive

Zeolites are known to be slow release fertilisers. Plant nutrients such as nitrogen and potassium are held by the negatively charged clinoptilolite structure and released on demand.Clinoptilolite application on the daily diet of the animals reduces digestion system illnesses. Clinoptilolite addition to the feed formulation has a positive effect on the growing up of the animals (Cadoso *et al*., 2011).

2.4.9. Fillers

Zeolites are used as fillers in the manufacture of papers. These filler grades of zeolite have a large potential for utilization in paint and plastics industries (Gustava *et al*., 2015).

2.4.10. Aqua Culture

Zeolites can reduce ammonium and hydrogen sulphide levels in fish/prawn ponds, resulting in increased fish/prawn growth rates and population densities. Zeolite is an efficient ammonia remover and also provides a large surface area for nitrifying bacteria in recirculation systems. Zeolites do not only provide optical clearness of your water but also keeps it biologically clean (Kwakye-Awuah, 2008).

2.4.11. Removal of Water Hardness

Water hardness is a measure of the concentration of Ca^{+2} and Mg^{+2} ions in water. Harder waters have higher concentrations of the ions and softer waters have lower ion concentrations. The unit used for quantifying water hardness is ppm Ca^{+2}, or mg CaCO3 per litre of water. The United States Geological Survey (USGS) uses the following scale to define the level of water hardness (see Table 2.1).

Table 2.1: Classification of Water hardness

Concentration of CaCO3	Classification
0-60 mg/L or 15 ppm – 50 ppm	Soft
61- 120 mg/L or 50ppm – 100ppm	Moderately Hard
121- 180 mg/L or 100 ppm – 200 ppm	Hard
181 -250 mg/L or > 200 ppm	Very Hard
>250 mg/L	Extremely Hard

(United States Geological Survey (USGS)

2.4.11.1. Economic and Health Effects of Water Hardness

Many chemicals found in drinking and Industrial water sources may be the cause of adverse human health effects, affect the acceptability of water uses for industry and lower the effectiveness of water treatment (Gesbrekidan and Samuel, 2011).

Water hardness is the traditional measure of the capacity of water to react with soap, hard water requiring considerably more soap to produce lather (Von Gunten, 2003). Hard water often produces a noticeable deposit of precipitate (insoluble metals, soaps or salts) in containers, including "bathtub ring". It is not caused by a single substance but by a variety of dissolved polyvalent metallic ions, predominantly calcium and magnesium cations, although other cations (aluminium, barium, iron, manganese, strontium and zinc) also contribute. Hardness is most commonly expressed as milligrams of calcium carbonate equivalent per liter. Water containing calcium carbonate at concentrations below 60 mg/l is generally considered as soft; 60–120 mg/l, moderately hard; 120–180mg/l, hard; and more than 180 mg/l, very hard (Li *et al*., 2012).

The hardness of water has less health effect, but it has a great economic problems both at domestic and industrial levels; for example domestically it cause wastage of soap during washing and formation of scales on cooking material and also since it increases the boiling point of water it results consumption of energy and fuel. At industrial level it is causing high economic effect on industries. For instance the followings are major problems related to water hardness at industries level.

Textile industry: the hardness and impurities present in the water affects the color, brightness and interferes with the texture of fabric produced and uniformity in colors dyed.

Dyeing industry: Textiles need to be dyed in order to get the required color. The water used during this process should be soft and free from organic matter. If hard water is used uniform dyeing is not possible because hard water decreases the solubility of acidic and basic dyes and dyes even precipitate out in such water that form unwanted spots or shades on the fabric and organic matter imparts foul smell.

Starch industry: Hard water causes precipitation of salts which accumulate in the starch. This reduces the adherence of the starch o the fabric thus reducing the efficiency

Sugar industry: Water containing sulphates, nitrates, alkali carbonates etc., if used in sugar refining, causes difficulties in the crystallization of sugar from molasses. It also causes the formation of precipitate which accumulates in the refined sugar. Moreover, the sugar so-produced may be deliquescent.

Paper industry: The hardness and impurities present interfere in the colour, texture and uniformity in papers and Calcium and magnesium salts increase the ash content of the paper, also tend to react with chemicals and other materials employed to provide a smooth and glossy (shining) finish to paper.

Pharmaceutical industry: Hard water, if used for preparing pharmaceutical products, may produce certain undesirable products in them. This will affect the efficiency of the drug and sometimes be hazardous. In large number of industries, water is used for the production of steam in boilers. The water thus used is called as boiler feed water. The

boiler feed water should be free from dissolved Calcium and magnesium salts Li *et al*., 2012).

The common methods used for removal of the metals of earth alkaline from aqueous solutions and softening of water can be classified as chemical precipitation, ultrafiltration, reverse osmosis, electrodialysis, adsorption, and ion exchange (Manio, 2000). Water softening using electrochemical techniques has gained attention and the packed bed of polypyrrole/polystyrene sulfonate electrodeposited porous carbon electrode has been used for continuous water softening from flowing artificial hard water solutions (Saleh, 2009), as well as Sand, limestone, marble, salt, clay, natural and synthetic zeolites are also some examples of nonmetallic minerals that have been used as water softening method.

Zeolites are inorganic crystalline aluminosilicates with a network of pores classified as microporous materials (pore size < 2 nm). In recent years, the class of zeolites and related microporous materials has been greatly expanded. These materials are of particular interest, both in the industry and in academia, due to their large variety of properties and areas of applications. These applications are growing continuously spanning from adsorption and separation to heterogeneous catalysis, and, nowadays, also in green chemistry (Li *et al*., 2012).

Considerable progress has been made in this dynamic field of research, with an emphasis on understanding the interplay of physicochemical properties, such as structure, composition, texture, and morphology, with the corresponding properties and behavior in the applications and industrial methods for synthesizing zeolites usually involve use of chemical grade reagents as starting materials and crystallization from a gel or clear solution under hydrothermal conditions. Nevertheless, preparation of synthetic zeolites from chemical reagent-grade sources of silica and alumina is costly (Gostuvaa *et al*., 2015).

The cost-effect concern has called the attention of researchers to seek cheaper raw materials for zeolite synthesis; many studies have focused their attention to the use of low cost aluminosilicate raw materials in order to reduce costs of the final zeolite products.

Nonmetallic minerals such as clays and diatomites can serve as aluminosilica sources for the production of synthetic zeolites with an adapted pre-treatment procedure (Gostuva *et al*., 2015).

Zeolites are used in huge quantities in a large number of industrial applications. For instance, zeolite A is used as a softener in phosphate free detergents (20-25 % of detergent composition and this is the largest application (in tons) of any zeolite and thus represents a huge market. Zeolite Y is used in the fluid catalytic cracking (FCC) process in oil refineries to convert heavy feedstock's to gasoline. This is the largest application of a zeolite as catalyst. Zeolites A and X are also used for gas drying in the industry (Zoller and Sosis, 2008). .

The study conducted in Ethiopia revealed that, the dominant sources of drinking water and Industrial water supply for major urban and rural communities are from wells and springs (Gebrekidan and Samuel, 2011). Hence, Water quality is a key aspect of urban and rural water supply, which may influence community attitudes, thereby potentially affecting the sustainability of water supply systems. Perceived poor water quality influences the use of water as well as the end products of the industries, thus creating potentials of health risks and economic problem through the development of unsafe alternative sources (Hoko, 2008).

2.5. Zeolite Synthesis

The synthetic zeolites are used commercially more often than natural zeolites due to the purity of crystalline products and the uniformity of particle sizes. The sources for early synthesized zeolites were standard chemical reagents. Much of the study of basic zeolite science was done on natural zeolites. The main advantages of synthetic zeolites in comparison to naturally-occurring zeolites are that they can be engineered with a wide variety of chemical properties and pore sizes and that they have greater thermal stability (Win, 2004).

The zeolite synthesis involves the hydrothermal crystallization of aluminosilicate gels (formed upon mixing an aluminate and silica solution in the presence of alkali hydroxides

and/or organic bases), or solutions in a basic environment. The crystallization is in a closed hydrothermal system at increasing temperature, autogenous pressure and varying time (few hours to several days). The type of the zeolite is affected by different factors such aging time and crystallization time and temperature (Lijalem *et al*., 2015).

2.5.2. Factors affecting Zeolite synthesis Parameters

2.5.2.1 Aging process

Ageing is the period between the end of the preparation of aluminosilicate gel and the crystallization process to increase the crystal growth by increasing the number of nuclei present in the aluminosilicate gel. In other words, the ageing period allows the aluminosilicate gel to reorganize structurally and chemically, which leads to an increase in the nucleation sites necessary for zeolite nucleation. Slangen*et al.* investigated the effect of ageing time on the microwave synthesis of Na-A zeolite (Slangen *et al*.,1997).They concluded that the short aging time of five minutes led to an amorphous material, whereas complete synthesis of zeolite Na-A was achieved successfully after an aging time of 20 h by increasing the degree of crystallization.

2.5.2.2. Crystallization process

Crystallization can be described as a process in which solid crystals are formed from the gel that consists of the source materials (Bronić *et al*., 2008). In this process, the molecules in the solution are transformed and arranged in a defined and organized pattern of crystals that can be controlled by the operating conditions. The two major crystallization process stages are the formation of crystals (nucleation) and the growth of the crystals. The nucleation process is initiated when unstable nuclei form in the solution of source materials, and these nuclei become larger and more stable over time, forming the crystals. The nucleation step includes both heterogeneous and homogeneous mechanisms. Many studies have expressed the fact that homogenous nucleation is preferable over heterogeneous nucleation, despite the fact that heterogeneous nucleation occurs more commonly. The homogeneous mechanism, which is more difficult to achieve than the heterogeneous mechanism, refers to the coverage of this process through

the surface and the interior structure of the substance. Conversely, the heterogeneous nucleation takes place at preferential sites, and it occurs more often than the homogeneous mechanism. The nucleation step is of a great importance, because crystal growth cannot be achieved without it. In other words, crystal growth can take place at any temperature below the melting point as long as nucleation exists.

In zeolite synthesis, the operating conditions during the synthesis process have a major role in the final formation of the desired zeolite structure. In general, there are many common conditions that have been highlighted for the majority of zeolite types, i.e., aging period, crystallization period, temperature, and the operational pressure. In 2008, Bronić*et al*. conducted a study to investigate the mechanism of zeolite A crystallization. They concluded that both the aluminosilicate gel and the crystalline phase occurred in different amounts during the crystallization process and that the amorphous aluminosilicate was dissolved completely after its formation, depending on the crystallization temperature. Thus, the crystallization time depends mainly on the crystallization temperature, because it affects the mechanisms of nucleation and growth. Generally, the crystallization time decreases as the operating temperature increases. Therefore, there is an inverse relationship between the crystallization period and the operating temperature (Strathmann *et al*., 2011).

2.5.3. Procedure for synthesizing zeolite

Zeolite synthesis involves producing a reaction mixture. Occurring in the synthesis mixture at the reaction temperature is the formation of zeolites from amorphous materials. The mixture undergoes nucleation usually at high temperature. The gel formed in the reaction process and the species in solution rearrange from continuous changing phase of monomers and clusters. Crystallization occurs after nucleation (Hu *et al*., 2017). In a typical aluminosilicate zeolite synthesis, sodium aluminate is dissolved in water along with some fraction of the additional sodium hydroxide that is needed for the reactant mixture. Separately, sodium silicate is mixed with the remainder of the sodium hydroxide. The two solutions are combined using the required mixing order and agitation level, resulting in the initial zeolite gel. In some cases this initial gel is aged at an

intermediate temperature for a time to allow evolution of the gel chemistry and perhaps initial nucleation of the system. The reaction mixture is then digested at a higher temperature usually between 50 and 200 ˚C for a prescribed time until the desired level o product crystallinity is reached (Kulprathipanja, 2010).

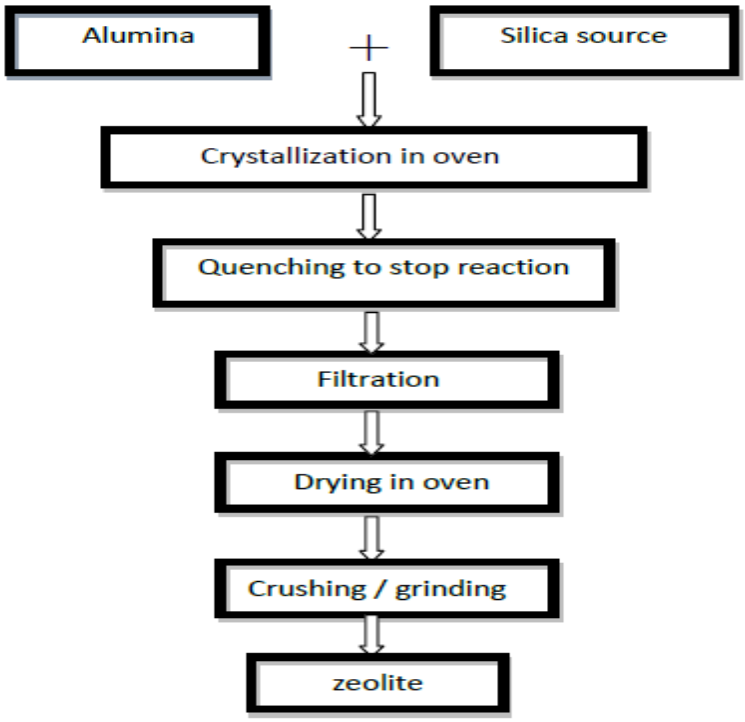

Figure 2.4: Flow Chart showing Zeolite Synthesis

As indicated in Kulprathipanja (2010) the order of mixing the reagents into the final slurry or gel can be critical. One order of mixing may give coarse slurry while a reversed order of mixing of the same reagents may give a thick gel. Nadir (2006) also emphasized that the important point in the synthesis process is the preparation of the synthesis mixture. A variation occurred in process parameters changes the product properties, moreover the product. Therefore, the composition and the homogeneity of the synthesis mixture, chemical nature of the reactants, crystallization temperature and the period, the template molecule, and pH of the system are the main factors affecting the zeolite synthesis.

2.5.4. Zeolite Precursor and Source Materials

Basic reactants and templates are used as starting components for synthesizing zeolites. In the basic reactants, an aluminium source, a silicon source, and water are generally used as the reactants for the synthesis process (Breck, 1974). In this process, as mentioned earlier, the zeolite framework depends mainly on the silica and alumina in building the primary units of the structure, while the water acts as the solvent during the synthesis process. Generally, water is used in these processes because it is capable of dissolving most of the ionic compounds that are used at the conditions of the process. The low viscosity of water makes it a good medium in which the reaction can take place, resulting in metastable phases with considerable crystal growth and various shapes (Cai *et al*., 2008). However, some compounds are insoluble in water, even at supercritical conditions. Therefore, mineralizer, such as sodium carbonate, sodium borate, and sodium sulphide, are added to enhance the solubility of the solute. As mentioned earlier, this process is conducted using a pressure vessel (autoclave), because the temperature and pressure have major influences on the formation and growth of crystals. Many substances have been used extensively as sources of silica, e.g., alkali silicate solution (sodium silicate), colloidal solution, fumed silica, tetraalkylorthosilicate, and some minerals (kaolin, Pumice and clays) and some industrial by products (Filter Cake and Bagasse Ash).

Alumina sources can be provided by alkali aluminate solution (sodium aluminate), aluminium sulfate solution, and hydrous aluminium oxides (pseudo boehmite, aluminium alkoxides). In the chemical industry, numerous source materials like templates are used to integrate the basic reactant of the synthesis preparation. There are two categories of templates in the zeolite industry, which means organic and inorganic templates, and both are used to enhance the desired zeolite structure. The importance of the templates is evident in the crystallization process and in the final structure formation of the zeolite. Many reports have indicated that both aqueous alkaline solution and templates are very important in zeolite structure formation. Templates lead to a process that occurs during nucleation to provide the initial building blocks of the structure by allowing both organic and inorganic species to organize the oxide tetrahedra into a specific geometrical

topologies around themselves. There are many types of templates including cations (Li^+, Na^+, K^+ and Ca^{2+}) and organic templates (tetrapropyl ammonium). The selection of the template to be used usually depends on the ability to remove the template without affecting the structure of the zeolite (Parnham and Morris, 2007).

In general, there are two main methods for zeolite synthesis using solid wastes as the silica–alumina source. The methods are widely recognized as single step and two step method. The single step method aims to utilize whole part of the silica contained solid waste for zeolite production without any separation. Usually this method employs hydrothermal treatment in a single pot for all preparation sequences that means dissolution of silica and alumina from the bulk solid in alkali solution and then re-crystallization of the two components into zeolites covering the undissolving solid. By employing this method there will be no leftover residue, however particles irregularities and crystal variety in the end zeolite products become the major drawbacks of this method. On the other hand, the two step method requires solid residue separation after most of silica and alumina content have been dissolved in the alkali solution. The residue removal increases the possibility in producing a desired type of zeolite with high purity and particle regularity (shapes and sizes) but leaving a new solid waste along with very low production yield. Meanwhile for eliminating any waste generation, a combination between the two methods has been proposed to produce high purity zeolites from the supernatant and also low grade zeolites from the mixture of the solid residue and the spent reaction mixture (Purnomo *et al*., 2012).

2.6. Characterization Methods of Zeolite

2.6.1. Powder X-Ray Diffraction (XRD)

X-ray diffraction (XRD) is widely utilized to elucidate the structure of crystalline materials (Lijalem *et al*., 2016). It is a technique used to confirm the structural characteristics of a synthesized specimen providing with a unique fingerprint of samples under investigation. XRD is based on the principle of scattering phenomena, whereby crystals perform the function of diffraction grating toward an incident X-ray. The atoms in the crystals scatter the X-rays in all directions (Xue *et al*., 2013).

The diffraction of X-rays in crystals was discovered in 1912 at the University of Munich by Max Theodor Felix Von Laue which earned him a Nobel Prize for Physics in 1914. In his work, he showed that X-rays are electromagnetic radiation of short wavelength similar in dimension to those of the bond distance in crystals which can act as a diffraction grating for incoming X-rays (Lijalem *et al*., 2016).

English physicists Sir W.H. Bragg and his son Sir W.L. Bragg developed a relationship in 1913 to explain why the cleavage faces of crystals appear to reflect X-ray beams at certain angles of incidence. They described for a crystalline solid that the waves are scattered from lattice planes separated by the interplanar distance d and the path difference between two waves undergoing constructive interference is given by $2d\sin\theta$, where θ is the scattering angle (Treacy and Higgins, 2001).

This leads to Bragg's law which describes the condition for constructive interference from successive crystal crystallographic planes (hkl) of the crystalline lattice which is given by the equation: $2d\sin\Theta = n\lambda$

This is called Bragg's law; n is generally taken as unity, d is the interplanar spacing of the atoms, λ is the wavelength of the incident X-ray. Crystalline materials contain infinite number of lattice planes and of different Miller indices, and hence various d-spacing can be calculated from the modification of the Bragg equation for any crystal system. A diffraction pattern is obtained by measuring the intensity of scattered waves as a function of scattering angle. Very strong intensities known as Bragg peaks are obtained in the diffraction pattern when scattered waves satisfy the Bragg condition. Using the Bragg peaks it is possible to calculate the crystallinity of crystals. Therefore studying the diffraction of X-ray is used to generate information about the structural properties of any crystalline material (Santasnachok *et al*., 2015).

2.6.2. Scanning Electron Microscopy

Scanning electron microscopy (SEM) is one of the most versatile instruments available for the examination of the morphology of solid materials including kaolin and zeolites. The configuration of a typical SEM shows that it is made up of an electron gun situated

on the top of the column which generates an electron with energy level in the region of 0.1-30 eV (Lijalem *et al*.,2016).

A high vacuum is usually provided to aid electron transport without interference or scattering by air. An electron beam scanning coil and signal detection system are also needed for the image processing of the sample surface. SEM works under the principle of interaction between the specimen and the electron beam producing a signal from secondary electrons and backscattered electrons which can be used to produce images. Secondary electrons are electrons produced when the incident electron beam collides with a sample atom electron and knock it out of its shell. It is weak in energy (nearly 100volts). Backscattered electrons are electrons formed when the incident electron beam collides with a nucleus of a sample atom and it bounces back out of the sample as a backscattered electron. These electrons have high energies and because a sample with a higher density will create more of them, they are used to form backscattered electron images, which generally can discern the difference in sample densities (Robson, 2001).

SEM consists principally of an electron gun, electron lenses, scan coils and detectors. The electron gun generates a beam of electrons from a cathode or filament usually made of tungsten. The electrons escape at high voltage from the filament. The final size of the beam is controlled by the electron lenses. Scan coils make the beam scan over the sample or target. When the electrons hit the target, they collide with electrons in the inner atomic shells. Back scattered and secondary electrons that escape from the sample are detected. If there is no detection, the image will be black (Ohrman, 2000).

2.6.3. Thermo gravimetric Analysis

Thermal or thermo gravimetric analysis measures the physical or chemical changes in a material. The temperature at which zeolites are dried has been suggested to have an effect on its structural characteristics (Trif *et al*., 1993). This is usually studied through thermal analysis. Thermal analysis is usually a group of techniques in which the physical property of a substance is and/ or its reaction products are measured as a function of temperature when the substance is subjected to a controlled temperature variation and data correlated

gives information about properties such as thermal stability, moisture content or solvent and decomposition temperature and rate.

2.6.4. Atomic Absorption Spectrometry (AAS)

Atomic absorption spectrometry (AAS) is an analytical technique that measures the concentration of an element. It is the process involving the absorption of light by free atoms or ions of an element at a wavelength specific to that element (Lijalem *et al*., 2015). In atomic absorption spectroscopy, emission, absorption and fluorescence energy is put into the atom population by thermal, electromagnetic, chemical and electrical forms of energy and is converted to light energy by various atomic and electronic processes before measurement. It is useful not only for the identification but also for the quantitative determination of many elements present in samples. The technique is specific, in that individual element in each sample can be reliably identified and it is sensitive, enabling small amounts of an element down to parts per billion of a gram in a sample (Lijalem *et al*., 2015).

3. Materials and Methods

3.1. Chemicals and Instruments

The following instruments were used during the research. X-ray diffractometer (Schmaduze.7000), Thermal analyzer (Schmaduze-60H), SEM, digital electrical conductivity probe, electronic balance, electrical oven, thermometer and a rotary shaker (L.E.D Orbit Shaker), AAS (Spectry-20 plus), Sieve Armfield CEN-MKII-00-A,PH-meter-PHscan10,Solid sample handling and Solid Mixer-armfield CEN-MKII-11, Muffle Furnance-AJEON.CO,LTD- Korea, Magnetic Stirrer-MS300HS were the apparatus used in this study.

Hydrochloric acid (HCl), Sodium hydroxide (NaOH, 98% lab Reagent Avi Chemindustries, Mumbia, India), Dihydrated Calcium Chloride ($CaCl_2.2H_2O$), Hepta Hydrated Magnesium Sulphate ($MgSO_4.7H_2O$),DiSodiumEDTA, Acetic Acid, Aluminum Oxide (Al_2O_3), Sodium Carbonate (Na_2CO_3) and Distilled water were all the chemicals used throughout the experiment, as well as the chemicals used were analytical grade and used without further purification.

3.2. Sample Collection

The Bagasse Ash used in this study was collected from Wonji Sugar Industry, Ethiopia. It was transported to Adama Science and Technology University on the same day and stored in laboratory for pretreatment and further characterization.

3.3. Sample Preparations

20g Bagasse Ash (BA) sample was sieved through a 75μm sieve. The sieved fine BA was divided into two equal amount and labeled as RBH and HBA. HBA sample was digested in 1M HCl to remove iron and washed with distilled water followed by drying overnight at 120 °C. Initial characterization of the RBA and HBA was carried out using XRD, whereas, the compositional analysis RBH and the thermal stability analysis of RBA and HBA were made by TGA/DTG.

3.4. Extraction of Bio-Silica from Bagasse Ash

The extraction of Bio-Silica was undertaken using the method described in Alves *et al*., (2017) and Thuadaij and Mukda, (2016). Accordingly, 1.0 g of Bagasse Ash was mixed with 1.3 g of NaOH in capsule and triturated to obtain a homogenized mixture. The mixture was then calcinated at 600 °C for 1h. After cooling to room temperature, the fused product was grinded then mixed with 100 ml distilled water to form suspension. The suspension was stirred for 24 h (120 rpm) at room temperature and resulting slurry was submitted to hydrothermal treatment at 90 ^{o}C for 20h.

The reaction product was filtered with a quantitative filter paper Whatman Number 41 and the filtered liquid (sodium silicate solution) was titrated with 3M Acetic Acid up to pH became 7. The resulting gel mixture was aged at 80 °C for 1 h (aging step). The gel was washed twice with 100mL of distilled water, filtered (sodium acetate solution), and separated from solid (silica gel). The silica gel was dried at 135 ^{o}C for 24h and kept in plastic container for characterization.

3.5. Synthesis of zeolite A

The synthesis of zeolite A from Bagasse Ash was carried out using the method developed by Hu *et al*., (2017), Lijalem *et al*., (2016) and Mohamed *et al*., (2017).

3.5.1. Synthesis Procedures

a) Preparation of $NaAlO_2$

$NaAlO_2$ required for molar ratio adjustment was prepared as follows:

$Na_2O_3 + Al_2O_3 \longrightarrow NaAlO_2$ (calcination at 1600 ^{o}C)

b) Preparation of intermediate products

$NaAlO_2 + BA \longrightarrow NaAlSiO_4 + Na_2SiO_3$. (Fused at 800 ^{o}C for 2h).

c) Gel formation

$NaAlSiO_4$+ Na_2SiO_3 + H_2O) (0.1:1w/v ratio) stirred at 50 ^oC for 1 h → Reaction gel

d) **Gel ageing**

The formed reaction gel was aged at room temperature for 0, 1, 3 and 12h.

e) **Hydrothermal Crystallization**

Crystallization → 80 **^oC,** 90 **^oC,** 100 **^oC** Zeolite A.

1, 3, and 12 h

Then, once the crystallization time was achieved, the reactors were removed from closed water bath and quenched in cold water to stop the reaction. The hydro gel pH was measured before and after the hydrothermal synthesis. The synthesized zeolite A was then washed with ultra pure distilled water until pH = 9 was attained in the wash water. Finally, the products were dried at 100 ^oC for 24 h. and coded as z-x-t-A.

Where: z is aging time, x is crystallization time, t is crystallization temperature and is two digit, BA-A is indicate Bagasse Ash derived zeolite A

The effects synthesis parameters were systematically studied by varying ageing time, crystallization time and temperature. The obtained result was coded as 0390-A, 1390-A, 3390-A, 1290-A, 3190-A, 31290-A, 3380-A, 33100-A and 3110-A the simplicity of the discussion, where number indicates ageing time, Crystallization time and temperature from left to right in each sample.

Lastly, for comparison standard zeolite A was searched by using ICDD file number from database in XRD schmaduze-7000) and percentage crystallinity of the synthesized Na-A zeolite was estimated as indicated in Rayalu *et al*., (2005) and 2^{nd}ed zeolite material synthesized, Harry,(2001) as follows:

$$\%Crystalli = XRD\ peak\ intensity\ of\ Sample \div XRD\ peak\ intensity\ of\ standard \times 100$$

Crystal size of the synthesized zeolite A was determined by using the Scherrer relation between line width and crystallite size as indicated in the literature part.

3.5.1. Characterization of Raw BA, Extracted Bio-silica and Synthesized Zeolite A

Characterization of BA and Na-A zeolite was carried out by using various characterization techniques.

3.5.1.1. Chemical Analysis

Analytic Chemical Analysis was conducted to determine the chemical composition of raw Bagasse Ash and Extracted Bio-Silica.

3.5.1.2. TGA/DTG Analysis

In this particular study, the thermal stability analysis of the starting raw bagasse Ash, HCl treated Bagasse Ash and Extracted Bio-Silica was carried out by using Thermal analyzer Schmaduze-60H instrument in the temperature range of 0-800 ^{o}C and at a heating rate of 20^{o}C/min by taking sample of 5 mg weight.

3.6.1.3. X-Ray Diffraction (XRD) analysis

The crystalline phase of Bagasse Ash, extracted Bio-silica and synthesized zeolite A were identified by powder XRD (Schmaduze-7000) using CuKα radiation (40 kV and 100 mA).The scanning rate was 0.06° s−1, and 2θ range is 0–80°.

3.5.1.4. SEM Analysis

The refined raw BA and synthesized zeolite A were sent to India for SEM analysis to study the morphology of raw Bagasse Ash and synthesized zeolite A and Sample preparation and instrument handling was conducted by a third party expert.

3.6. Water Softening

In order test water hardness removal capacity of the synthesized zeolite A, first 0.5 g/l hard water was prepared for each ion. Calcium solution was prepared by taking 1.8375 grams of $CaCl_2.2H_2O$ in 1L to get 0.5 gram/L of $Ca^{2+}$and that Magnesium was prepared by dissolving 5.1347 grams of $MgSO_4.7H_2O$ in 1 L to 0.5 grams/l of Mg^{2+} so that solutions with concentrations in a range equivalent to very hard water have been obtained (Adel et al; 2010).

Softening processes were carried out by using the synthesized zeolite A. The zeolite A capacity as cation exchanger, removing Ca^{2+} and Mg^{2+} and delivering Na+, was evaluated at 0.5g dose zeolite A, 100 ppm concentrations of ions, 2h contact time and 7 pH. Analyses of Atomic Absorption Spectroscopy were carried out in order to determine calcium and Magnesium concentrations in the solutions before and after treatment with zeolite A. From the synthesized zeolite A at different synthesis parameters the one with high removing capacity and high crystallinity percentage was selected for hardness removal optimization by varying dose of zeolite, concentration of Ca^{2+} and Mg^{2+} ions, Contact times as well as pH of the solution.

3.6.1. Effect of dose of synthesized zeolite

The effect of dosage was studied by varying zeolite A dose from 0.5 g to 1.5 g by increasing with 0.5 interval at fixed 200ppm metal ions concentration, 2 h contact time and 7 pH.

3.6.2. Effect of Ca^{2+} and Mg^{2+} ions concentration

The Ca^{2+} and Mg^{2+} ions removal experiments were conducted using synthetic hard water solutions prepared from Ca^{2+} and Mg^{2+} dissolved in distilled water. Beakers containing a mixture of 100 ml of 100 ppm , 150 ppm and 200 ppm Ca^{2+} and Mg^{2+} to optimize the metal ions concentration at constant 0.5 g dosage of zeolite A,7 pH and 2 h contact time.

3.6.3. Effect of Contact time

The influence of the contact time of Na-A zeolite on the hardness removal was investigated by varying the contact time from 1 h- 3 h at constant 0.5 g of zeolite dose, 200 ppm Ca^{2+} and Mg^{2+} ions concentrations and 7 pH value.

3.6.4. Effect of pH

The effect of pH was investigated by varying PH 6 to 9 by fixing dose synthesized zeolite to 0.5g,contact to 2h and concentration of Ca^{2+} and Mg^{2+} ions 200ppm. In all case the mixtures were shaken at room temperature for 2 h on orbital shaker at 500 rpm. All experiments were conducted at room temperature in 200 ml beakers then after the solutions were filtered and their concentrations determined were measured in ppm after $LaCl_3$ was added as reagent directly from Atomic Absorption spectroscopy against the blank solution at specified wavelength metal ions and each measurement was carried out with triplicates and the measurement with small Ds value was taken (Loiola *et al*., 2017).

The percentage removal of the synthesized zeolite was calculated as follows:

$$\%\ \text{Removal} = \frac{(C_0 - C_e)}{C_0} x100$$

Where, % Removal is the ratio of the difference in calcium and magnesium concentrations before and after hardness removal.

The amount of calcium and magnesium ions adsorbed q_t and q_e were calculated as follows according to the following equation (Peric et al; 2004)

$$q_t = \frac{V(C_0 - C_t)}{M}$$

$$q_e = \frac{(C_0 - C_e)V}{M}$$

Where, q_e and q_t are the removing capacities (mg g^{-1}) of the calcium and magnesium ions at equilibrium and at any time respectively. And C_0, C_t and C_e are initial concentration,

concentration at any time and equilibrium concentrations of the Ca^{2+} and Mg^{2+} ion in aqueous solutions (mg L^{-1}) respectively, V is volume of the solution (L), and M is mass of the dry zeolite A (g).

3.7. Adsorption isotherms and Kinetic

3.7.1. Adsorption Isotherm

Adsorption isotherms which are very important in describing the adsorption behavior of solutes on specific adsorbents were examined with the obtained experimental data. The removal Ca^{2+} and Mg^{2+}ions with different initial concentrations were analyzed by using the models given by Langmuir and Freundlich which correspond to homogenous and heterogeneous adsorbent surfaces, respectively. 0.5 g/L of zeolite Na-A was introduced to 50 ml of Ca^{2+} and Mg^{2+} ions solution with 100 ,150 and 200 mg/L initial concentrations at pH = 7 for 120 min.

3.7.1.1. Langmuir isotherm

The sorption behavior of Ca^{2+} and Mg^{2+} on Na-A zeolite surfaces was followed using the Langmuir isotherm and Freundlich isotherm models. The Langmuir model is valid in the case of the monolayer adsorbed Ca^{2+} and Mg^{2+} ions onto zeolite surface. The well known linear expression of the Langmuir model is given by:

$$\frac{Ce}{qe} = \frac{1}{qmb} + Ce/qm$$

Where, q_e (mg/g) is the adsorbate amount adsorbed on adsorbent at equilibrium and C_e (mg/L) is equilibrium adsorbate concentration in solution. The parameters q_m (mg/g) and b (L/mg) are the Langmuir constants that relate to the maximum adsorption capacity and energy of adsorption respectively. To check whether it fits to Langmuir isotherm, it is by looking some parameters like. A further analysis of the Langmuir equation can be made on the basis of a dimensionless equilibrium parameter R_L, known as the separation factor as given by

$$R_L = \frac{1}{1+bC_o}$$

Where C_o is initial adsorbate concentration (mg/l) and b is Langmuir constant (l/mg). The value of R_L indicates the type of isotherm as follows (EL-Mekkawi *et al*., 2015).

Table 3.1: type of isotherm for R_L parameter

R_L	Types of Isotherm
$R_L=0$	Irreversible
$0< R_L<0$	Favorable
$R_L= 1$	Linear
$R_L> 1$	Unfavorable

3.7.1.2. Freundlich isotherm

Freundlich model explains the relation between qe and equilibrium Ca2+ and Mg2+ concentration is give by the following equation:

$$lnqe = lnKF + \frac{1}{n} lnCe$$

This sorption model assumes the multilayer capacity and usually is applied to the highly heterogeneous surfaces (Cardoso *et al*., 2011).

Where KF (mg/g) is an indicator of the multilayer adsorption capacity and 1/n is the adsorption intensity and indicates both the relative distribution of energy and the heterogeneity of the adsorbent sites. The linear plot of lnqe versus lnCe at constant temperature gives intercept of values KF and slope 1/n respectively. When Ce equals unity lnKF is equal to lnqe. In the other case, when 1/n = 1, the KF value depends on the units in which qe and Ce are expressed. A favorable adsorption tends to give Freundlich constant, n value between 1 and 10. Larger value of n (smaller value of 1/n) implies strong interaction between adsorbent and lead ions while 1/n equal to 1 indicates linear

adsorption leading to identical adsorption energies for all the sites (EL-Mekkawi *et al*., 2014).

3.7.2.2. Kinetic Studies

Equilibrium study is important in determining the efficiency of adsorption. Several kinetic models are used to explain the mechanism of adsorption processes. These models include Pseudo-first-order rate model and Pseudo-second order rate model (Hu *et al*., 2017).In the present work, kinetic data obtained from batch studies have been analyzed by using pseudo first order and pseudo second order in order to clarify the adsorption kinetics of calcium and magnesium ion onto zeolite Na-A.

3.7.2.1. Pseudo-first-order model

Lagergren's equation is the one most widely used (Upenyu *et al*., 2017) for the adsorption of solute from an aqueous solution. The pseudo-first-order kinetic equation may be written as:

$$\log(q_e - q_t) = \log(q_e) - \left(\frac{K_1}{2.303}\right) t$$

Where q_e and q_t (mg/g) are the amounts of calcium and magnesium ions adsorbed at equilibrium and at time t, respectively, and K_1 is the kinetic constant of pseudo-first-order adsorption (min^{-1}).

3.7.2.2. Pseudo-second order model

The pseudo-second-order equation (Upenyu *et al*., 2017) is expressed as follows:

$$\frac{t}{q_t} = \left(\frac{1}{q_e}\right) t + \frac{1}{k_2 (q_e)^2}$$

Where $\mathbf{q_t}$ (mg/g) is the amount of calcium and magnesium ions adsorbed at time **t**, K_2 is the pseudo-second-order rate constant of adsorption (g/ (mg min)), qe is the adsorption capacity at equilibrium (mg/g) and **t** is the contact time (min). If the second order kinetic equation is applicable, the plot of t/q_t against **t** of above equation should give a linear

relationship. The q_e and K_2 can be determined from the slop and intercept of the plot $\mathbf{1/q_e}$ versus **t** respectively

4. Results and Discussion

4.1. Characteristics of Bagasse Ash

4.1.1. Chemical Composition Analysis of Bagasse Ash (BA) and Bio-SiO_2

The chemical composition of BA is shown in table 4.1. The major compositions of BA were SiO_2 (71.5%) and Al_2O_3 (8.16%). It also contains high amounts of iron oxide and calcium oxide and very minor quantity of TiO_2 and MnO. One of the positive aspects of these industrial byproducts is that they free of toxic leachable elements like Co, Cr, V, Cd, Ar, Pd. Additionally; BA contains some Na and K which should provide some charge stabilization to zeolite framework with some drawbacks include high percentage of unburnt carbon, iron oxide and calcium oxide.

Table 4.1: Chemical Composition of Bagasse Ash and Extracted Bio-SiO_2

Oxides	Bagasse Ash (wt %)	Bio-SiO_2
SiO_2	71.50	25.54
Al_2O_3	8.16	1.43
Fe_2O_3	5.12	0.80
CaO	1.68	<0.01
MgO	1.24	<0.01
Na_2O	1.60	18.04
KO	5.80	1.16
MnO	<0.01	0.04
P_2O_5	0.68	0.18
TiO_2	0.34	<0.01
H_2O	1.23	21.42
LOI	3.59	32.47
SiO_2/Al_2O_3	14.9	
Na_2O/SiO_2	0.023	

The BA can be classified as F-class medium grade based on a standard called ASTM C-618 is used for the classification Table 4.2 below shows the comparison of BA with ASTM C-618 standard.

Table: 4.2. BA comparison and standardization

Properties	BA %	ASTMC618 requirement %
SiO_2+Al_2O_3+ Fe_2O_3	84.78	70 (minimum)
SO_3	-	5 (maximum)
LOI	3.59	6 (maximum)

The finding is in agreement with the chemical composition of other wastes that have been re-used at different countries (Alves *et al*., 2017).

The chemical composition of extracted Bio-Silica was also presented in Table 4.1. Chemical compositional analysis of extracted bio-silica result showed that the produced biosilica had high percentage of SiO_2 (25.54%). However, it was almost free of Fe_2O_3, CaO, MgO, MnO, P_2O_5 and TiO_2 oxides. Moreover, the chemical composition analysis result showed there was high percentage of Na_2O than that of RBA. This fact suggests that the titration with Acetic Acid was not completed silica content of the sample is in sodium silicate solution pure Bio- Silica SiO_2. Therefore, to get only pure Bio-Silica form the sample should be titrated with Acetic Acid up to pH reaches 7. In order to reduce the H_2O and LOI of the extracted Bio-Silica it must be calcinated above 550^oC.

This property may be beneficial for the use of the prepared gel in many environmental and industrial applications. The result is similar with reported of Thuadaij and Mukda, (2016) in which Bio-silica was extracted from Buriram sugarcane bagasse ash for synthesis of zeolite A.

4.1.2. Thermal Analysis of BA

Figure 4.3 displays the Thermogravimetric and differential thermal analyses (TGA/DTA) of RBA, HBA and B-Silica. The HBA thermogram presented a weight loss up to 100^oC

was corresponds to the loss of physically adsorbed water from the surface and the second step (521.94◦C) was related to the loss of the unburnt organic structure and that of without acid treatment sample mass loss was described 370.16 ^{o}C and 460.15 ^{o}C that related the loss of physically adsorbed water from the surface (Gursova *et al*., 2015 sand Sales and Lima, 2010) and the exothermic peak at 500^{o}C (DTA) evinces the existence of organic residues. Thus, the treatment up to 550 ^{o}C removes all undesired organic compounds (OC) to extract the bio-silica from BA and the zeolite synthesis. These results are in good agreement with report of Alves *et al*., (2017).

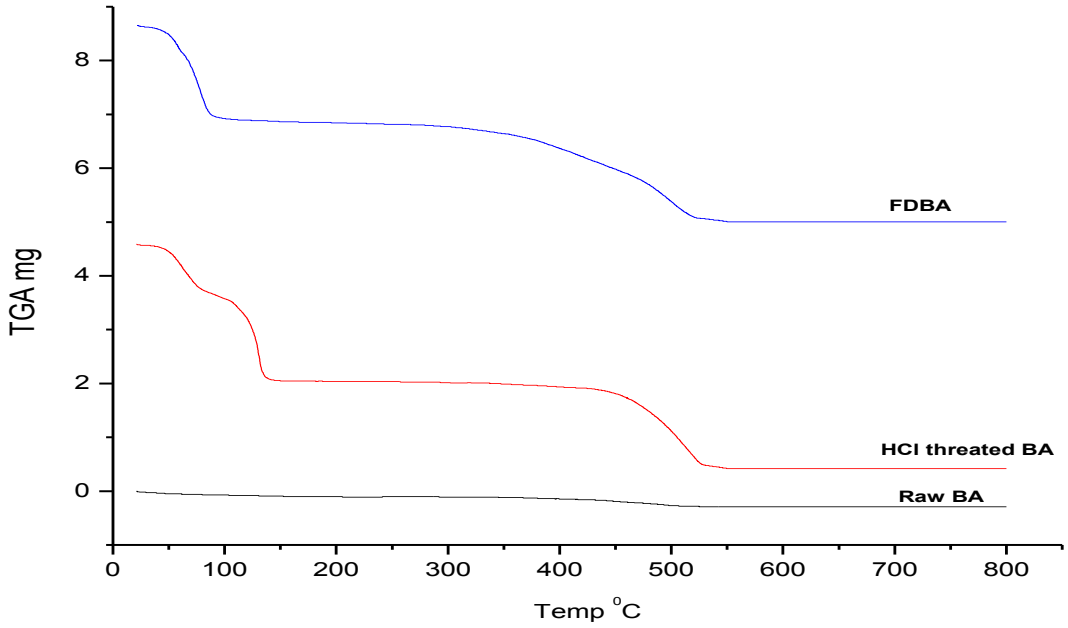

a) TGA

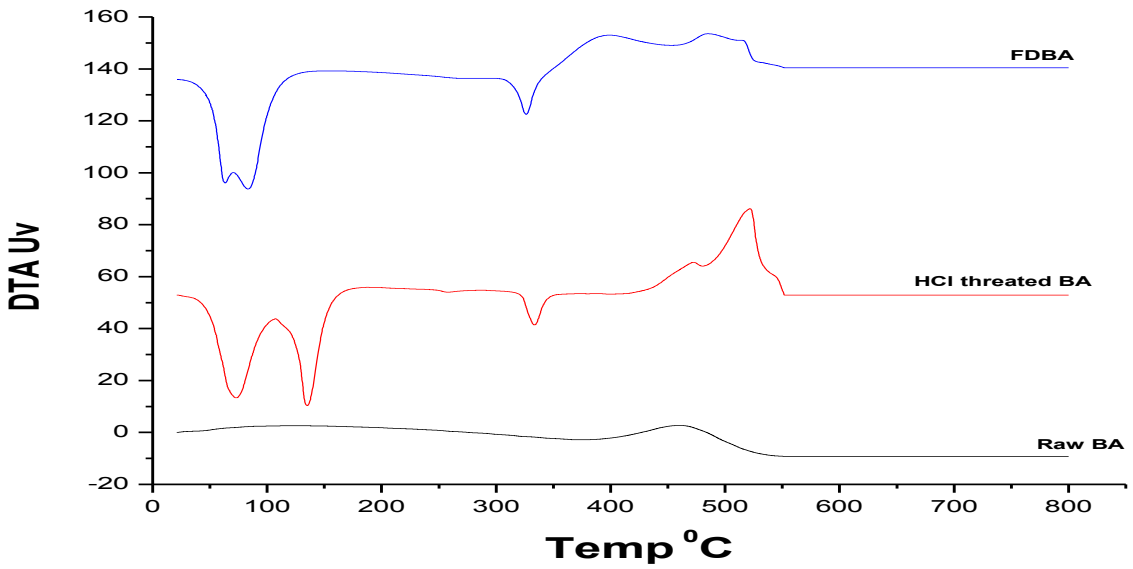

b) DTA

Figure 4.1: Thermogravimetric and differential thermal analyses (TGA (a)/DTA (b) of Bagasse Ash and extracted Bio-silica.

Again Figure 4.1 indicates the Thermogravimetric Analysis and Differential Thermal Analyses (TGA/DTA) of Bio-Silica indicates. A weight loss around 100 ^{o}C and 521.94 $^{\circ}$C was related to mass loss of physically adsorbed water from the surface the loss of the organic structure (CH_3COONa) respectively (Gustavo *et al*., 2015).

4.1.3. XRD Analysis of RBA and H BA

The XRD patterns of RBA (Figure 4.2) indicated the presence of silica only in the crystalline phase that the peaks observed at 26.81°, 35.98°, 17.8°, 39.4^{o}, 40.2°, 42.5°, 45.8°, and 50.2° are typical of quartz. This result was indicated that sample is matched well with result reported by Alves *et al*., (2017) and as mentioned in Le Blond *et al* report the crystalline phase of silica in the BA is related to the conditions of combustion (mainly time and temperature). For example at temperatures of 500–800 $^{\circ}$C or when the exposure to high temperature is small, the silica contained in the Bagasse Ash is predominantly amorphous. At temperatures greater than 800 $^{\circ}$C, the amorphous silica present in Bagasse Ash is converted in crystalline silica polymorphs, such as quartz,

cristobalite and tridymite (Le Blond *et al*., 2010). One of the reasons for the peaks of quartz and mullite around 26 to almost overlap is due to presence of SiO_2 components in both quartz and mullite crystals. Moreover, the HBA sample become more crystalline than the RBA, this might be due the conversion of metallic oxides of were changed into the soluble Chloride form of this metals. Therefore to increase the percentage of SiO_2 in RBA sample, it is advisable to digest RBA in specified concentration of HCl. This result is similar with the previous work that reported by Patcharin *et al*., 2009 in which the silica content of similar solid waste was increased with increasing the combustion temperature and after treated with HCl.

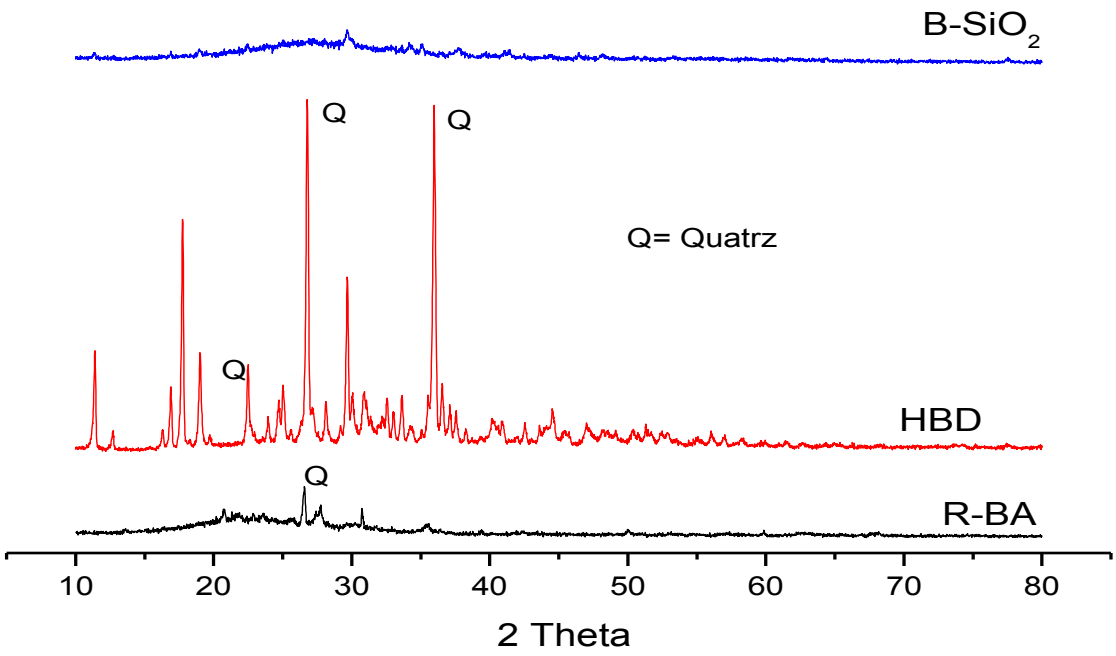

Figure 4.2: XRD patterns for raw Bagasse Ash (R-BA), HCl treated Bagasse Ash (HBD) and Extracted Bio-silica (B-SiO_2).

Figure 4.2 also tells us the XRD pattern of extracted Bio-Silica. As indicated the in Figure the broad X-ray diffraction peak at 2Θ degree confirmed the formation of amorphous silica, in general (Alves *et al*., 2017).

4.1.4. SEM Analysis of Bagasse Ash

SEM micrograph of BA (Figure 4.3) seems like fibrous material containing large shallow pores with strands in each fold. The morphology of the BA as observed in the micrograph of Figure 4.2 are similar to those presented by Denise *et al*., (2014).

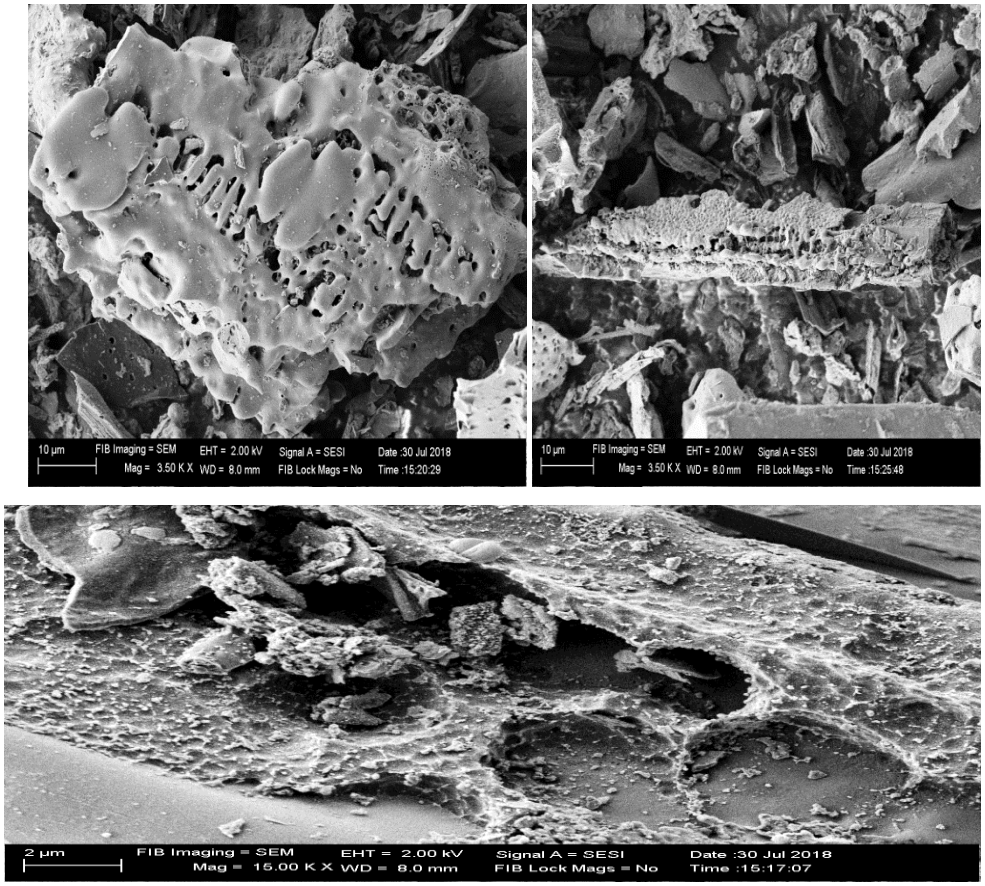

Figure 4.3 SEM image of RBA (Source: Taken from Yishak current Thesis)

4.3. Characteristics of synthesized zeolite A

4.3.1. $NaAlO_2$

As aforementioned in Table 4.1 section 4.1.1 the molar ratio of SiO_2 and Al_2O_3 ($SiO_2/A_2O_{3)}$ was 14.9 and that of Na_2O/SiO_2 was 6.8. This implied that eventually BA not satisfied the requirement for the synthesis of zeolite A. Thus molar ratio of SiO_2/ Al_2O_3

and Na_2O/SiO_2 in BA sample was corrected with $NaAlO_2$ which was prepared by calcinating Na_2CO_3 and Al_2O_3 and it was served as source of Al_2O_3 and Na_2O.

4.3.2. Characteristic of intermediate product ($NaAlSiO4$ and Na_2SiO_3) and 3390-A

Figure 4.4 (CM) shows the XRD patterns of product obtained from calcinated mixture of BA and $NaAlO_2$. The XRD pattern confirms the formation of $NaAlSiO_4$ and Na_2SiO_3 as intermediate product for the synthesis zeolite A. This is in good agreement with previous finding of Jiang *et al*., (2016). The XRD profile of the synthesized product Figure 4.4 3390-A showed that the previously peaks of $NaAlSiO_4$ and Na_2SiO_3 were disappeared and peaks of zeolite A were appeared at 2Ɵ degree 29, 98, 37.87, 34.16, 35.14 and 23.96 values as the major peaks of zeolite A (Harry, 2001).

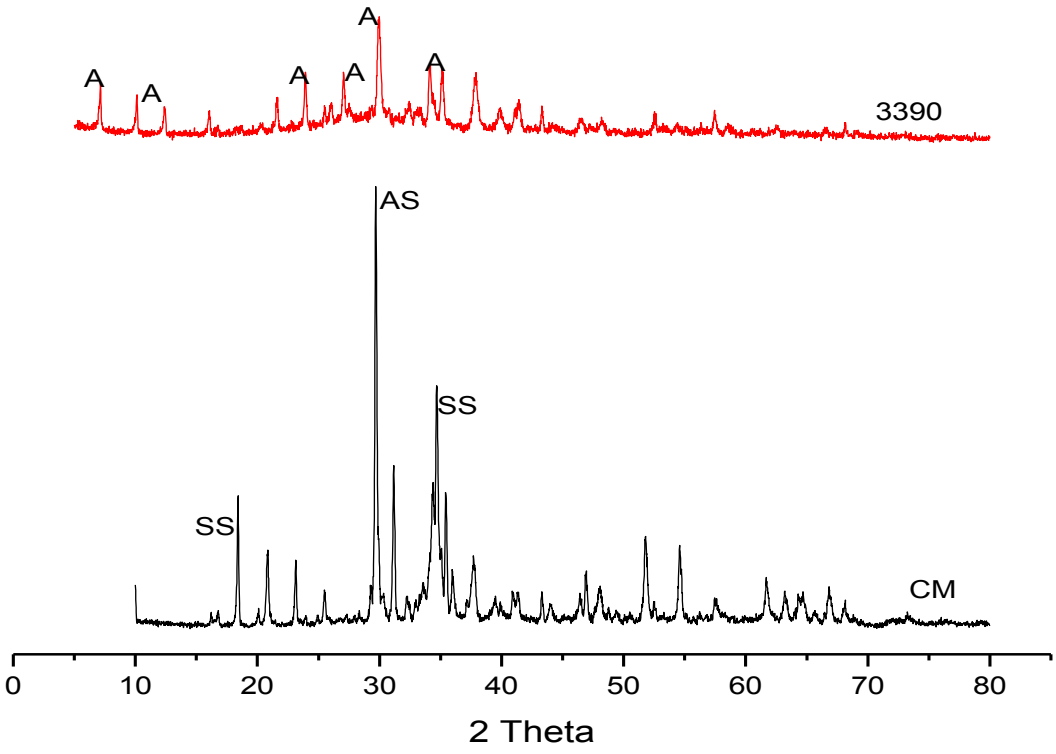

Figure 4.4 XRD patterns of intermediate products (bottom or CM) and Pre-synthesized Na-A zeolite (top). (SS= Sodium Silicate, AS= Aluminum Silicate).

Table 4.4 shows the estimated $\%C_{XRD}$ of sample 3390-A by taking the sum total of relative intensities of ten individual characteristic peaks with the sum total of relative intensities of ten individual characteristic peaks of standard.

Table 4.4: Ten Characteristic peaks and their relative intensities and % CXRD of SA and 3390-A

peak 2Ɵ	I for SA	I for 3390-A	% CXRD for SA	%CXRD for 3390-A
29.950	100	100	100	57.34
24.010	95.8	44		
7.210	73.9	32		
27.130	80.3	39		
10.205	58.1	25		
34.165	60.9	54		
21.680	57.6	27		
12.490	47.1	22		
16.130	37.2	5		
26.095	25.9	17		

SA= Standard zeolite A , I= relative intensity,3390-A zeolite A synthesized at 3h ageing time,3h at 90^{o}C crystallization time and temperature respectively.

The appearance of totally nine peaks and 57.34% crystallinity for the sample was the promising result for synthesis zeolite A from BA and also result was in good agreement with the findings in Hu *et al*., (2017). However, the %CXRD of synthesized zeolite was low as compared with % CXRD of standard zeolite (Table 4.4)**.** This might be due to the incomplete dissolution of both silica and alumina into solution and existence of unreacted silica and alumina which hinder the formation of the preliminary building blocks. Thus aluminosilicate gel was not reorganized chemically and structurally to form the zeolite structure (Zhang et al., 2013).

4.3.3. SEM Analysis of 3390-A (zeolite A)

Figure 4.5 displays the surface morphology of the 3390-A sample obtained using SEM images with different magnifications. The 3390-A zeolite particles with size 1 to 3μm were grouped into clusters to form cubic shape with rounded edge as expected. This particular morphology and particle size of zeolite A is suitable for the particular application as a cation exchanger (Upenyu *et al*., 2017)

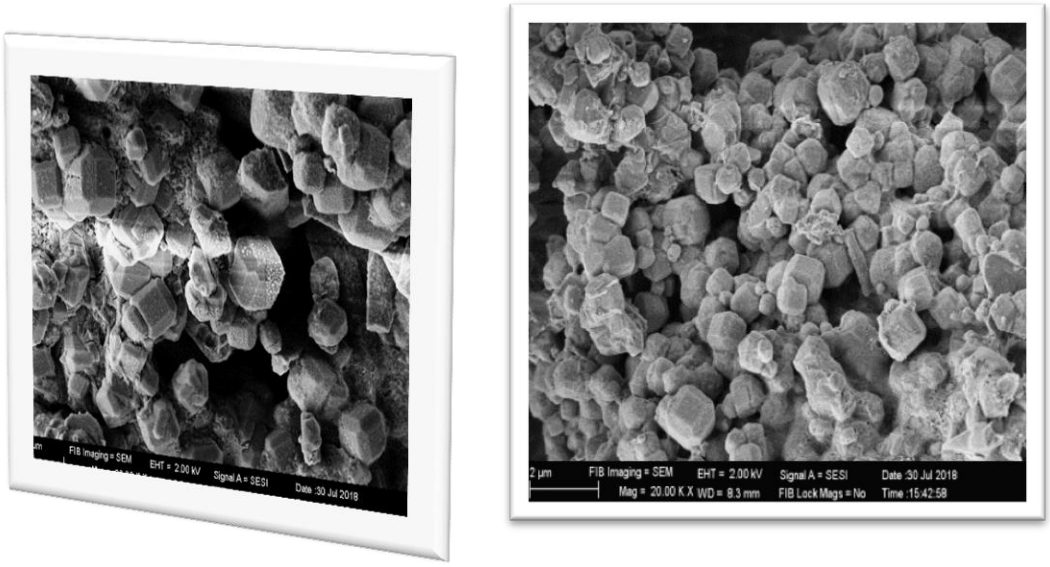

Figure 4.5: SEM images for 3390-A at different magnifications.

Additionally, no considerable amount of amorphous materials was detected by this technique, which indicates the crystallization manner (3h and 90 ^{o}C) that described in this work is advantageous as a cost-effective alternative to produce zeolite (Figure 4.5).

4.3.3.1. Effect of gel aging time

Figure 4.6 indicates the effect of ageing time on crystallinity of synthesized zeolite A. The relative percent crystallinity (% C_{XRD}) of 0390-A, 1390-A, 3390-A and 12390-A samples was calculated from the XRD profiles (Table 4.6).

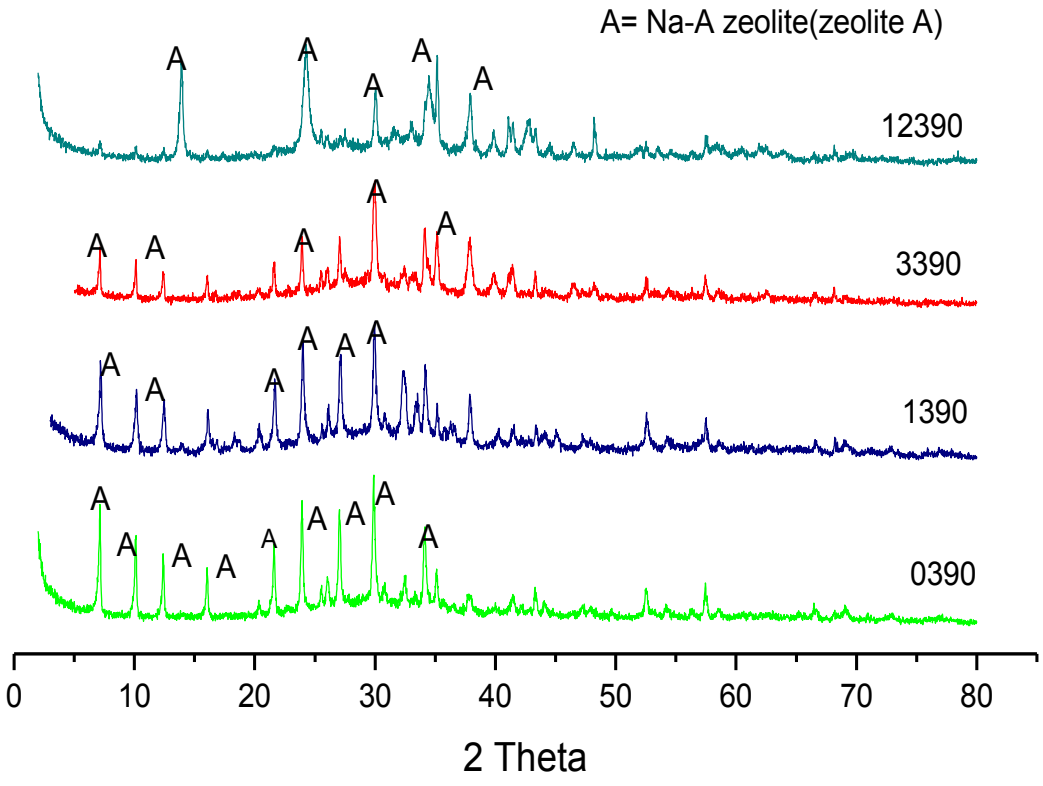

Figure 4.6: XRD patterns Na-A zeolite synthesized aged at 0 h (0390),1 h (1390), 3 h (3390) and 12 h (12390) times

XRD patterns clearly reveal that zeolite A with better crystallinity can be obtained as aging time is prolonged from 0h -12h. Table 4.6 shows the relative percent crystallinity (% C_{XRD}) calculated from the XRD profiles for the synthesized zeolite A aged at room

temperature followed by different aging time. This is because during aging period, both silica and alumina were completely dissolved into solution and reacted with each other to form some preliminary building blocks. Thus aluminosilicate gel is expected to reorganize chemically and structurally to form the zeolite structure during aging. Based on this, the study result showed that all the samples obtained were well crystallized. This justifies that the aging time does not markedly influence % C_{XRD} of the final end products because there was no high variation in % C_{XRD} of non aged sample (0390-A) and sample that was aged for 1h (1390-A) (Table 4.6). The result was found to be similar those results that reported earlier by Lijalem et *al*., (2016). But there is a decrement of % C_{XRD} the sample aged for 12h this might be due to the formation of pure zeolite A always relatively at short treatment time (Hu *et al*., 2017).

Table 4.6: %CXRD of zeolite A from BA at different ageing time

Sample	Aging time (h)	%C_{XRD}
0390-A	0	97.7
1390-A	1	97.8
12390-A	12	84.2.
3390-A	3	70.7

The crystal size distribution of samples obtained is shown in Table 4.7. As shown in this table zeolite A obtained with aging time of 0, 1, 3 and 12 h shows a mean crystal sizes of were 34.7, 30.7, 21.7 and 18.9 nm respectively. These results reveal that, for zeolite A synthesis under room-temperature conditions, longer aging time leads to the mean particle size of crystal decrease slightly. This can be explained by the fact that longer aging time would lead to more pre-nuclei (Gora *et al*., 1997). In general, aging at low temperature promotes nucleation process and increases the number of nuclei in the synthesis system because it offers the time required to achieve the formation of nuclei, which leads to the formation of smaller crystals. This critical effect of aging time on crystal size has a good agreement with a previous report using pure chemicals as the silica source (Zhang *et al*., 2013).

Table: 4.7. Effect of ageing time on crystal size

Ageing time (h)	**0**	**1**	**3**	**12**
Crystal size (nm)	34.7	30.6	21.2	18.9

4.3.3.2 Effect of Crystallization time

Figure 4.8 indicates XRD patterns of 3190-A, 3390-A, 3690-A and 31290-A samples that were synthesized at different crystallization times. Figure displays that most in all cases the characteristic peaks the synthesized zeolite A for different crystallization times were matched with the characteristic peaks of standard zeolite A at 2 theta values of 30.054, 24.106, 27.227, 7.365, 34.302, 29.977, 37.866, 34.166, 35.142, 23.932, 29.932, 23.980, 27.108, 34.165 and 21.662 degrees which is similar with what was reported by Treacy and Higgins, (2001).

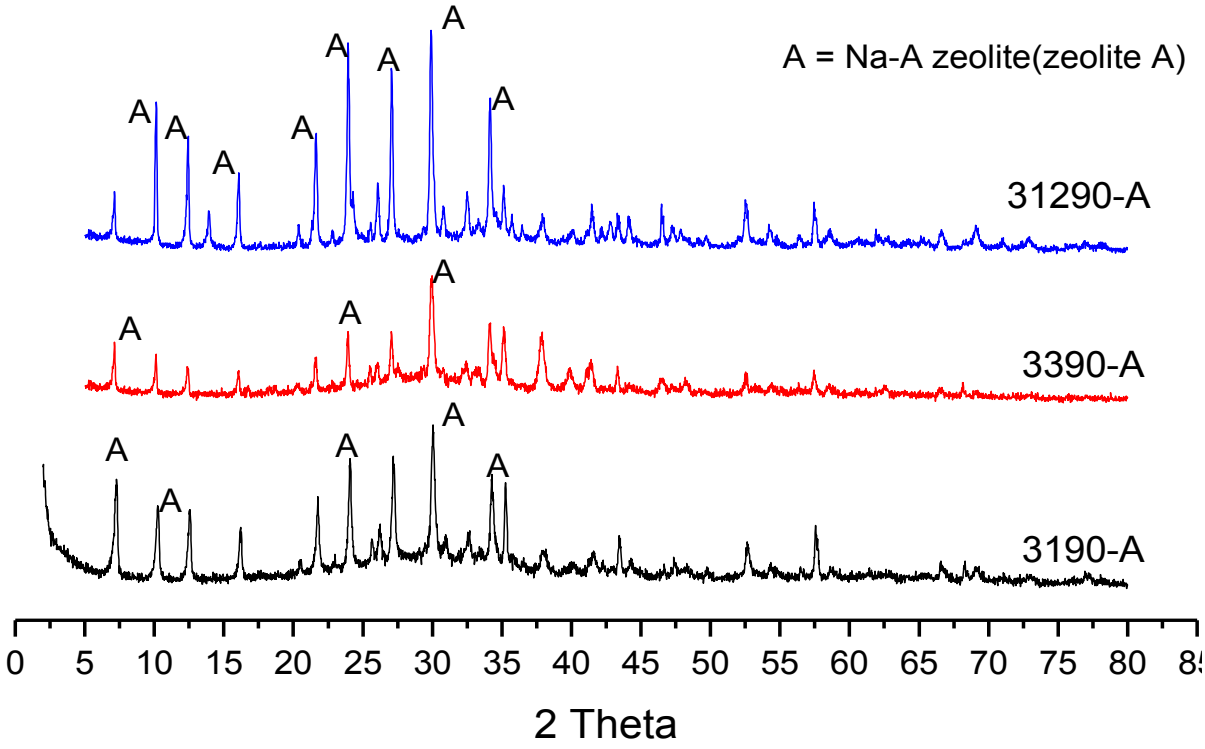

Figure 4.8: XRD patterns zeolite A synthesized at different time (1 (3190-A), 3 (3390-A) and 12 h (31290-A)).

Table 4.8 shows the % C_{XRD} of the synthesized zeolite A, in which the samples were found to exhibit decrement in % C_{XRD} from 1h to 3h.

% C_{XRD} was increased at 1h but there was the decrement of %C_{XRD} at 12h shows the formation of Na-X zeolite in addition to zeolite A in the reaction system (Zhang *et al*., 2013). All over, the result is in good agreement with works in Wang *et al*. (2008) that reported the structural formation of zeolite Na-X requires longer crystallization time due to it more complex and larger polymeric silicate units (D6R) and sparser structure rather than zeolite A, thus zeolite A was the main crystalline phase during the shorter crystallization time.

Table.4.8: %CXRD of zeolite A obtained at different time interval from BA

Sample	Aging time (h)	$\%C_{XRD}$
3190-A	1	98.5
3390-A	3	70.7
31290-A	12	86.0.

Table 4.9 shows the effect of crystallization time on crystal size the zeolite A. Among these samples, for 31290-A increasing synthesis time terminates formation of zeolite A crystals size (Table 4.9), because crystallinity and mean crystal size of zeolite A increases with increasing synthesis time for 1 h, but decreases for 12h (Table 4.8). The result confirms the range of zeolite A synthesis time is below 6h and disappearance of zeolite A at higher time (Lijalem *et al*., 2016).

Table 4.9 Effect of crystallization time on crystal size of synthesized zeolite A

Crystallization time (h)	**1**	**3**	**12**
Crystal size (nm)	27.7	21.7	34.7

Moreover, as zeolites are thermodynamically metastable phases. Successive reactions are followed in zeolite synthesis, a metastable phase appears first and then successively more stable phases are replaced with each other. For example, with prolonged crystallization time, Na-A zeolite is dissolved to form zeolite-sodalite (SOD), when synthesized in an alkaline aluminosilicate-gel (Denise *et al.*, 2014). In other words, increasing crystallization time causes dissolving of synthesized zeolites in the alkaline solution and as a result decreases crystallinity and crystal size. However, it must be mentioned that formation of zeolites cannot be rationalized on a thermodynamic basis alone and kinetics must be considered as well (Harry, 2001).

4.3.3.3. Effect of Crystallization Temperature

The figure 4.9 displays the effect of crystallization temperature on the crystallinity of zeolite A product from BA. Controlled experiments were carried out from 80 °C to 110 °C with the other conditions unchanged. The characteristic XRD peaks of zeolite A appear even after crystallization at 80 °C. However, these peaks are broad and short, showing the low crystallinity and purity of the product (Figure 4.10 3380-*A*). The XRD peaks are narrowed and sharp from 80 °C to 110 °C (Figure 4.9 3380-A – 33110-A*)* showing that in this temperature range, rising temperature would promote the crystallization of zeolite A and there is a positive correlation between the crystallinity of the zeolite product and the crystallization temperature (Table 4.10).

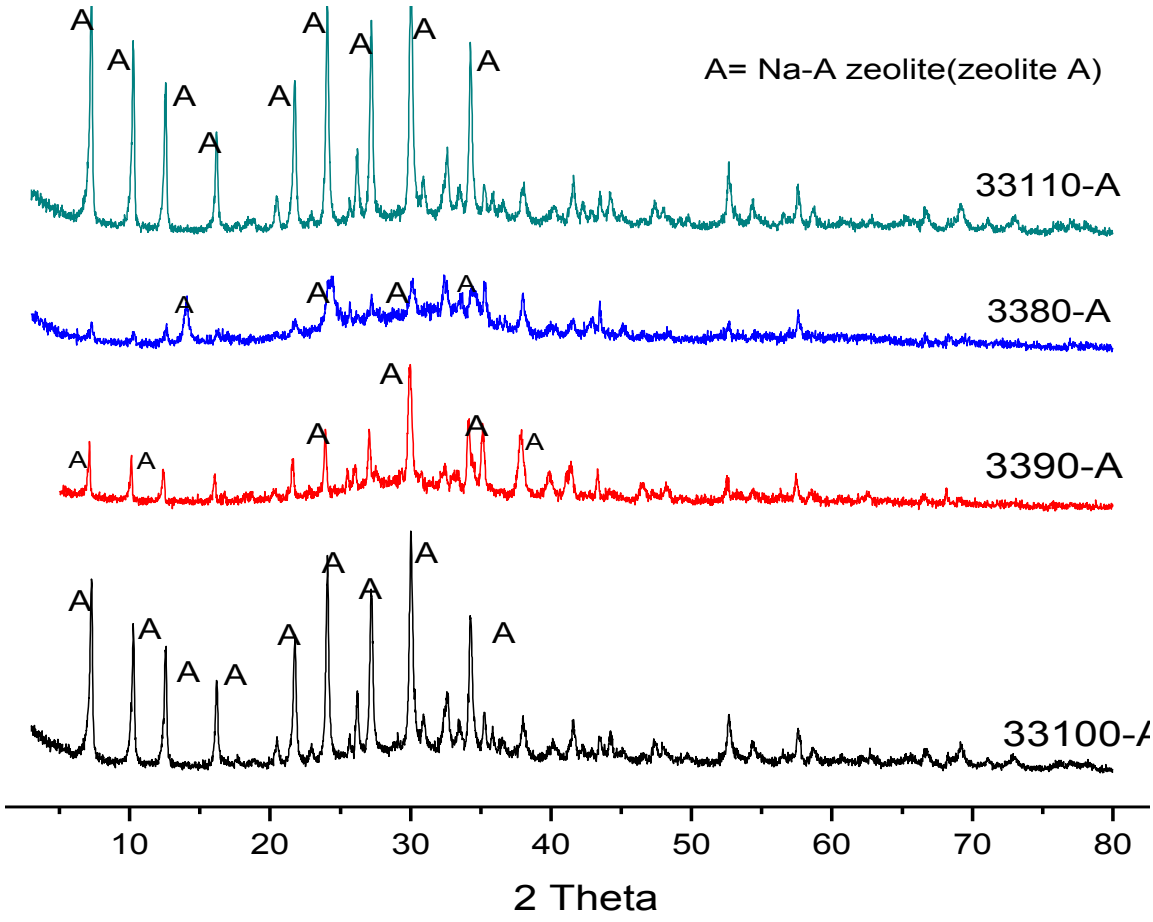

Figure 4.10: XRD patterns of zeolite A synthesized from BA at different temperatures (3380-A) at 80^{o}C, (3390-A) at 90^{o}C, (33100-A) at 100^{o}C, and (33110-A) at 110^{o}C**.**

Table 4.10: %C_{XRD} of zeolite A synthesized different temperature

Sample	Crystallization tep. (^{o}C)	% C_{XRD}
3380-A	80	80.0
3390-A	90	70.7
33100-A	100	97.7
33110-A	110	99.01

As zeolite A is thermodynamically less stable than sodalite (SOD) the appearance the peak that appeared around 56 ^{o} is one the indication for formation of SOD phase if would goes above 110^{o}C (Figure 4.10 and Table 4.8). This is because higher temperature will promote the conversion of metastable zeolite into a more thermodynamically stable phase Thus, to obtain pure-phase Na-A zeolite from Bagasse Ash and to lower the energy consumption for the synthesis, the crystallization temperature should be controlled in the range 80- 110 °C.

Table 4.11 presents the effect of crystallization temperature on crystal size of the synthesized zeolite A. Except at 80^{o}C (9.8 nm) a similar trend was observed for crystal size that increases with increasing synthesis temperature 21.7 to 34.7nm). Thus, it can be concluded that at these conditions, larger Na-A zeolite crystals can be produced with higher crystallinity at higher crystallization temperature. According to literature (Mirfendereski and Mohammadi, 2011), nucleation and crystal growth are strongly affected by crystallization temperature, because increasing temperature increases both nucleation rate and crystal growth rate. Thus, higher growth rates and larger crystals can be obtained at higher temperature as compared with other sample (Sapawe *et al*., 2013).

Table 4.11 Effect of crystallization temperature on crystal size of synthesized zeolite A

Crystallization Temperature (^{o}C)	80	90	100	110
Crystal size (nm)	9.8	21.7	32.4	34.7

4.3.3.4. SEM analysis of optimized synthesized Sample 3310-A (zeolite A)

Figure 4.11 shows SEM image of 33110 ^{o}C-A which was obtained after optimization of the synthesis parameters. The sample obtained is well shaped with cubic rounded edge

than the 3390-A sample. The increasing of crystallization temperature to 110 ^{o}C does markedly influence crystal size of the final end product as well as $\%C_{XRD}$ of the (Table 4.12 and Table 4.13). The result is in good agreement with reports of Mirfendereski and Mohammadi, (2016) in which the increasing synthesis temperature from 80 to 100 °C significantly increases crystallinity of zeolite-Na-A and formation large size with cubic structure.

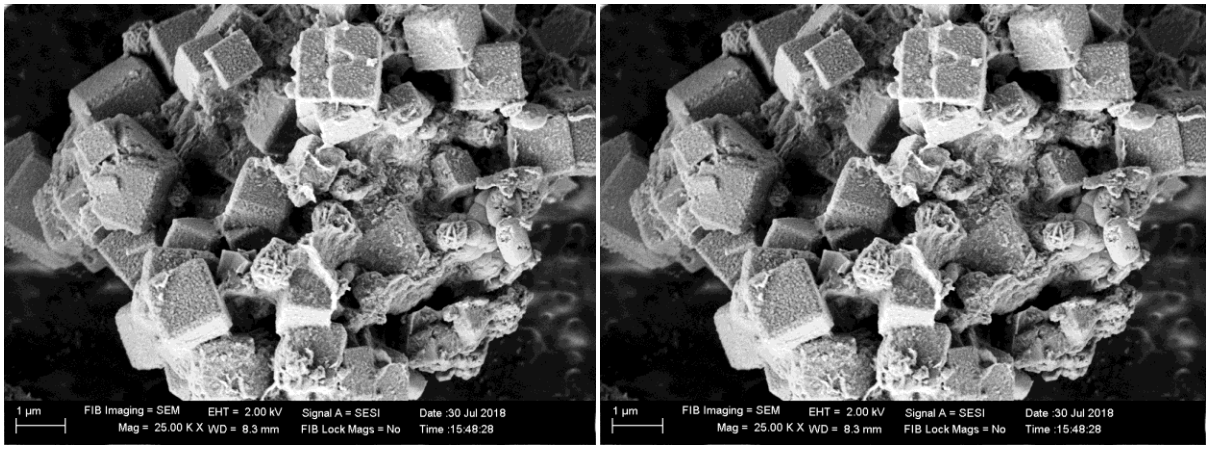

a) **b)**

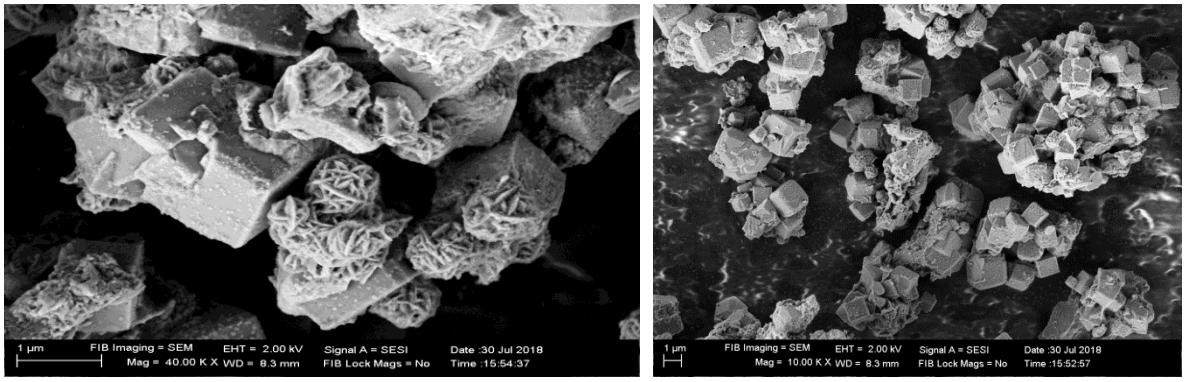

c) **d)**

Figure 4.12: SEM images of Na- A zeolite synthesized at 3h, 3h and 110 ^{o}C aging time, crystallization time and temperature respectively and at different magnification.

However, some literatures justified that increasing crystallization temperature may result the formation mixture of zeolites rather than pure zeolite A and zeolite A with irregular

shape, this is might be due the transformation initially formed zeolite A into hydroxysodalite because of a higher concentration of sodium in the liquid phase due to evaporation of water occurs during hydrothermal treatment (Ismail *et al*., 2010).

Table 4.12: Ten Characteristic peaks and their relative intensities and % CXRD of standard zeolite A and optimized zeolite A.

peak 2Ɵ	I for SA	I for33110-A	% CXRD for S**A**	% CXRD for 33110-A
29.950	100	100	100	93.75
24.010	95.8	86		
7.210	73.9	84		
27.130	80.3	77		
10.205	58.1	66		
34.165	60.9	64		
21.680	57.6	55		
12.490	47.1	4		
16.130	37.2	35		
26.095	25.9	26		

SA= Standard zeolite A , I= relative intensity,33110-A zeolite A synthesized at 3h ageing time,3h at 110 ^{o}C crystallization time and temperature respectively

In general, Figure 4.11 and Table 4.12 show us, the synthesis using the Bagasse Ash, gel formation at 50 °C stirring for 1h and aging the reaction gel for 3 h followed by 3 h and

110 ^{o}C crystallization resulted in an optimum crystallinity of about 93.75%. Moreover, in this particular product the numbers of crystals is larger and have better uniformity compared to the other products at different synthesis optimization discussed above.

4.6. Water Softening

Table 4.13 indicates the water hardness removing capacity of nine synthesized zeolite A from BA at different synthesis parameters. All samples reduced both ions except sample 3390-A and 1390-A for Ca^{2+} , a high reduction Ca^{2+} was observed by sample 33110-A, 0390-A and 3380-A (96.5 %,95.4 % and 95.2 %) respectively, the observed variation was might be due to the initially used water.

The case was however different for Mg^{2+} and Ca^{2+}, both ions showed a decrease in their concentrations when sample 33110-A was added to the synthetic hard water.

Table 4.10: Water softening capacity, % C_{XRD} and Crystal size of Na –A zeolite from BA

Sample	% CXRD	Aver. Crystal size (nm)	Meta Ion Binding Capacity (ml/g/g)	
			Ca^{2+}	Mg^{2+}
33110-A	99.01	34.7	500ml/g/g	83ml/g/g
3190-A	98.5	27.7	20ml/g/g	50ml/g/g
1390-A	97.8	30.7	-	73ml/g/g
0390-A	97.7	34.7	494ml/g/g	82ml/g/g
33100-A	97.7	32.4	493ml/g/g	71ml/g/g
3380-A	80.0	9.8	18ml/g/g	109ml/g/g
31290-A	86.0	34.4	117ml/g/g	65ml/g/g
12390-A	84.2	18.9	76ml/g/g	85ml/g/g
3390-A	70.7	21.7	-	38ml/g/g

Considering the removal efficiency and its % C_{XRD} (Table 4.12), sample 33110-A was the best to remove water hardness for 3h contacting time, 3h ageing time and at 110 ^{o}C of a major role on the crystallinity of synthesized zeolite A, On the other hand water hardness removing efficiency increase as % C_{XRD} of synthesized increase A, all of the results observed follow the work pioneered by Rayalu *et al*., (2005).

In general, from the XRD, % C_{XRD}, SEM micrographic analyses and removal efficiency of the sample 33110-A (zeolite A) were confirmed that 3 h crystallization time, 3h aging time at room temperature and 110 ^{o}C crystallization temperature are the optimum synthesis conditions for synthesis zeolite A from BA for its application of water hardness removal **(**Table 4.12 and Appendices**).**

4.6.1. Effect of dose of synthesized zeolite A

Figure 4.13 displays the effect of synthesized zeolite doze on removal of water hardness caused by Ca^{2+} and Mg^{2+}. The effect of amount of adsorbent on the uptake of Ca^{2+} and Mg^{2+} was examined. Ca^{2+} and Mg^{2+} ions removed versus amount of zeolite showed that the removal of the metal ions increases with an increase in the amount of zeolite (Mohamed *et al*., 2017). For Calcium and Magnesium, there was a substantial increase when the dose of zeolite was increased from 0.5 to 1.5 g because there were more sites for the adsorbate to be adsorbed. The increase in the removal efficiency was not so significant when the zeolite amount was further increased as could be seen from Figure 4.13 because competition for bonding sites between molecules of the adsorbate decreases with increase in the dosage of the adsorbent.

According to the Figure 4.12 better performances of the zeolite are achieved as its weight is increased (94.19 % to 96.43 % for Ca^{2+} and 78.00 % to 99.235 % for Mg^{2+}). The result obtained is similar to those presented by (Cinar and Baykal, 2005) and previous report of Loiola *et al*., (2012).

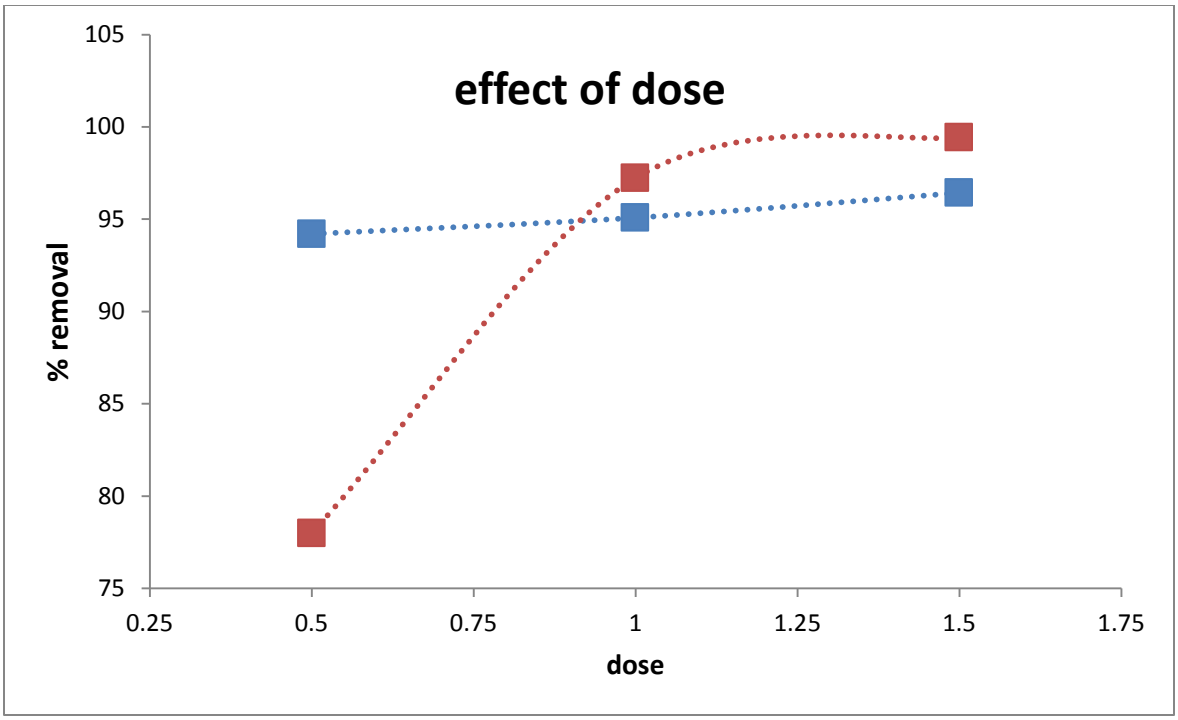

Figure 4.12: The effect of synthesized zeolite A dosage on the removal of Ca^{2+} (blue line) and Mg^{2+} (red line) (ions concentration =200 mg/L, volume of ions solution= 50ml, Time 2h, pH =7 and room temperature).

4.6.2. Effect of contact time

Figure 4.13 shows the adsorption capacity of Ca^{2+} and Mg^{2+}ion onto Na-A zeolite at different contact time. The effect of contact time on the adsorption of Ca^{2+} and Mg^{2+} was examined. The result for Mg2+ion showed that adsorption was rapid in the first 1h followed by a gradual increase with time until equilibrium was attained. For Ca^{2+} showed slight decrease in first 1h and increased again until equilibrium reached. The fast adsorption at the initial stage was probably due to the initial concentration gradient between the adsorbate in the solution and the number of vacant sites available on the adsorbent surface. The attainment of equilibrium adsorption might have been due to reduction in the available active adsorption sites on the adsorbent with time resulting to limited mass transfer of the adsorbate molecules from the bulk liquid to the external surface of adsorbent. The removal of Ca^{2+} ions reaches 95.53% at 3h while the maximum removal 99.78% removal was achieved for Mg2+ with fast rate 2h. The removal

percentage is merely the same at 2h and 3h. Removal percentage of Ca^{2+} ion at 3h shows a negligible increase (_±0.05%). Consequently, the optimum contact time of both Ca^{2+} and Mg^{2+} ion solutions with zeolite was set at 2h. The result was found to exhibit similarity with those reported earlier by Farrag *et al*., (2016).

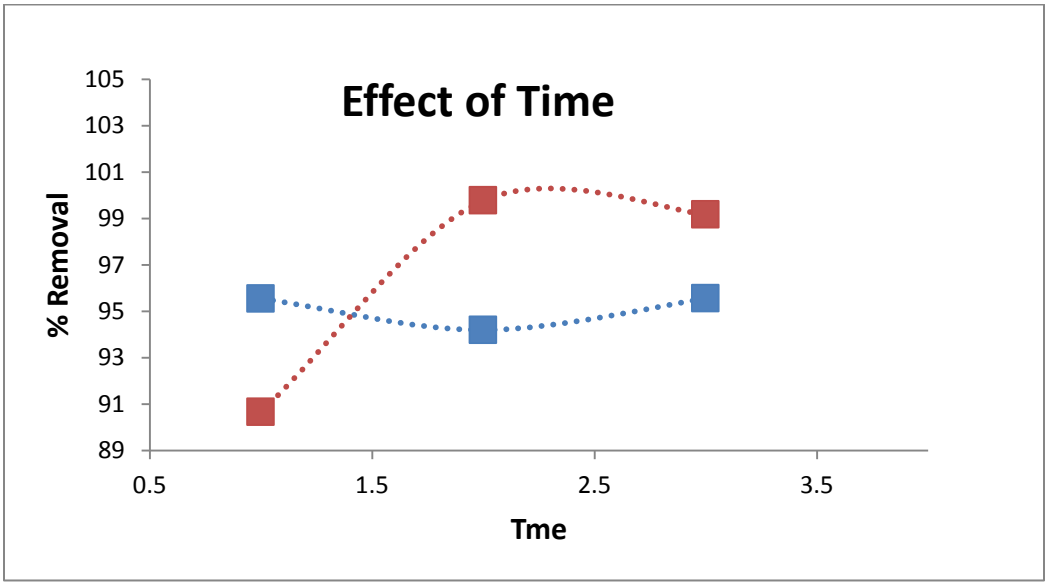

Figure 4.13: Change of the removal percentage of Ca2+ and Mg2+ ions at different time intervals. (Weight of zeolite= 0.5 g, Ca2+ and Mg2+ concentrations =200 mg/L, PH=7, volume of Ca2+ and Mg2+ solution =50 ml, T = 25± 0.1oC), (Ca=blue line, Mg= red line).

4.6.3. The effect of Ca^{2+} and Mg^{2+} ions concentration

Figure 4.14 presents the effect of concentration of Ca2+ and Mg2+ ions on removal of water hardness. Elucidating the removal mechanisms of Ca^{2+} and Mg^{2+} ions by the synthesized Na- A zeolite could be useful in the optimization process. In the light of previous studies, the removal process usually occurs through one or more of three mechanisms (EL-Mekkawi and Selim, 2014; EL-Mekkawi *et al*., 2015). The first is the ion exchange mechanism which involves a stoichiometric replacement of two mobile Na+ ions incorporated into zeolite pores and cages with one Ca^{2+} and Mg^{2+} ions from

solution. The second process is the adsorption of Ca^{2+} and Mg^{2+} onto zeolite sites probably occurring via the Van der Waals interactions. The third mechanism of Ca^{2+} and Mg^{2+} removal occurs via the precipitation of the ions as hydroxides.

The Ca2+ and Mg^{2+}concentration do not affect the synthesized zeolite efficiency. This finding is different from the result that observed in the commercial zeolite where the efficiency decreases as the Ca2+ concentration is increased, however, the result is in good agreement with Loiola *et al*.,(2012), who reported increasing concentration has no effect on the efficiency of the synthesized zeolite A from kaolin.

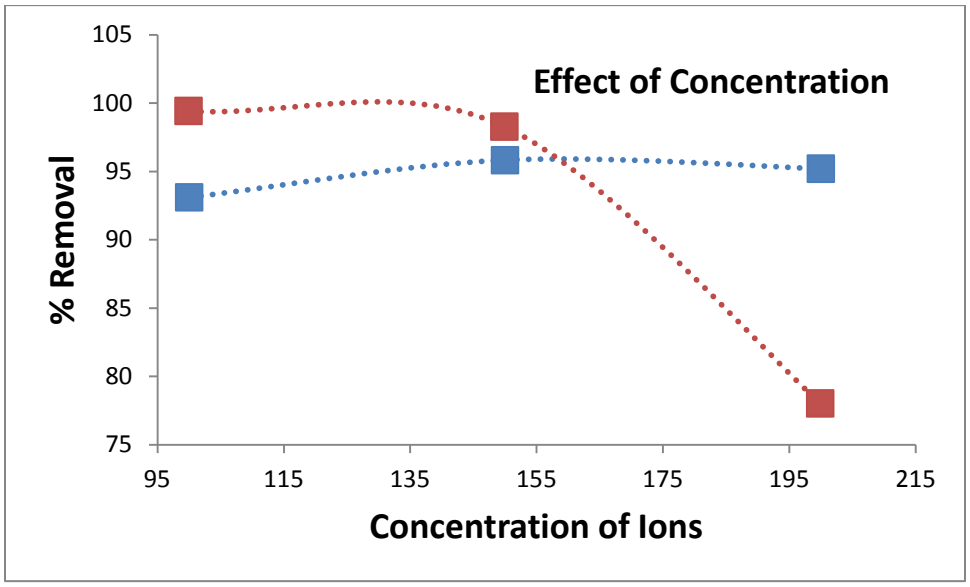

Figure 4.14: Change of the removal percentage of Ca^{2+} and Mg^{2+} ions at different concentrations of Ca^{2+} and Mg^{2+} (Weight of zeolite= 0.5 g, pH = 7, volume of Ca^{2+} and Mg^{2+} solution =50 ml, T = 25± 0.1^{o}C) (Ca= blue line, Mg= red line).

4.6.4. Effect of pH on Adsorption

Figure 4.15 shows the effect of pH over the efficiency of zeolite A in the process of water softening. In this study the effect of pH examined the removal of Ca2+ ion increased as pH value of the solution increases. For Mg2+ ion it reached maximum at pH 7, then showed slight reduction, then increase. This result shows the uptake efficiency depends on pH value and it can work in wide range of pH and as an explanation of Figure 4.17, at high pH, the surface charge of zeolite is more negative due to presence of OH^- groups that leads to formation of hydroxyl complexes. Formation of such hydroxyl compounds at higher pH is responsible for the uptake of the metal ions from the solution. Upenyu et al.,(2017) similarly reported that the removal of Ca2+ was increased as pH value increased from 4- 8.

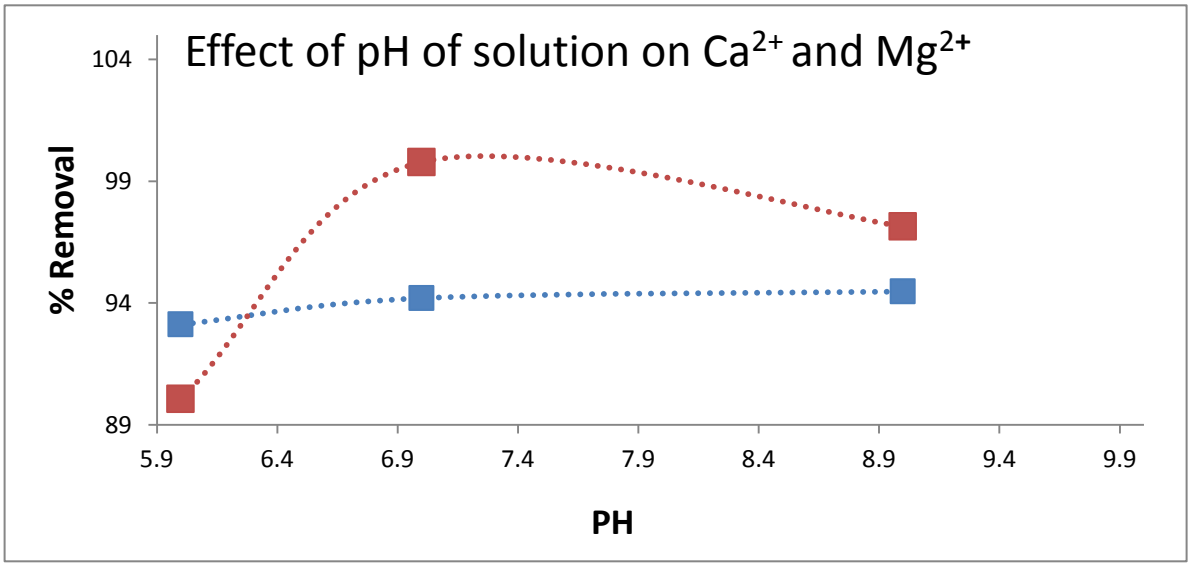

Figure 4.15: Change of the removal percentage of Ca2+ and Mg2+ ions at different PH value. (Weight of zeolite= 0.5 g, Ca2+ and Mg2+ concentration =200 mg/L, volume of Ca2+ and Mg2+solution =50 ml, T = 25± 0.1 oC), (Ca = blue line and Mg= red line).

4.7. Adsorption isotherm

Figure 4.16a, b the Langmuir, Figure 4.17a,b the Freundlich isotherm and Table 4.11 show adsorption data**.** Adsorption isotherms are very important in describing the adsorption behavior of solutes on specific adsorbents.

The plot of (Ce/qe) versus Ce showed that the experimental data fitted well in the linearized equation of the Langmuir isotherm over the whole Ca^{2+} and Mg^{2+} ions concentration range studied. Linear plots of lnqe versus lnCe showed that Freundlich isotherm was also representative for the Ca^{2+} and Mg^{2+} adsorption by zeolite A. A plot of lnqe versus lnCe enables the empirical constants K_f and 1/n to be determined from the intercept and slope of the linear regression.

In this study, Langmuir isotherm has a better fitting model than as the former have higher adsorption capacity in addition to close correlation regression coefficient than the latter thus indicating the applicability of monolayer coverage of the Ca^{2+} and Mg^{2+} ion on the surface of adsorbent as well as observed high removing capacity in this model, indicating the applicability of monolayer coverage of the Ca^{2+} and Mg^{2+} ions on the surface of newly synthesized product because application of the Langmuir equation involves the assumption that the surface is homogeneous (EL-Mekkawi and Selim., 2014).

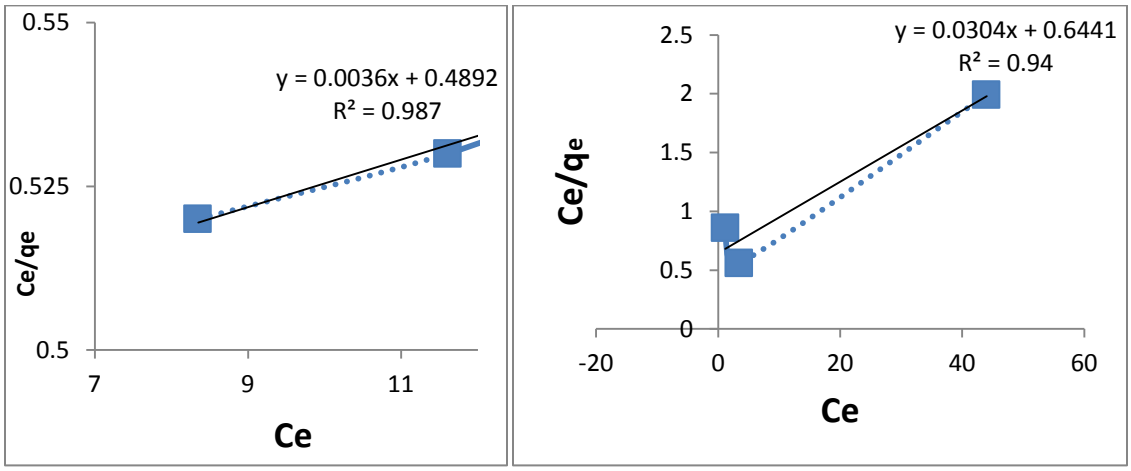

a) b)

Figure 4.16: Langmuir isotherm model For Calcium (a) and Magnesium (b).

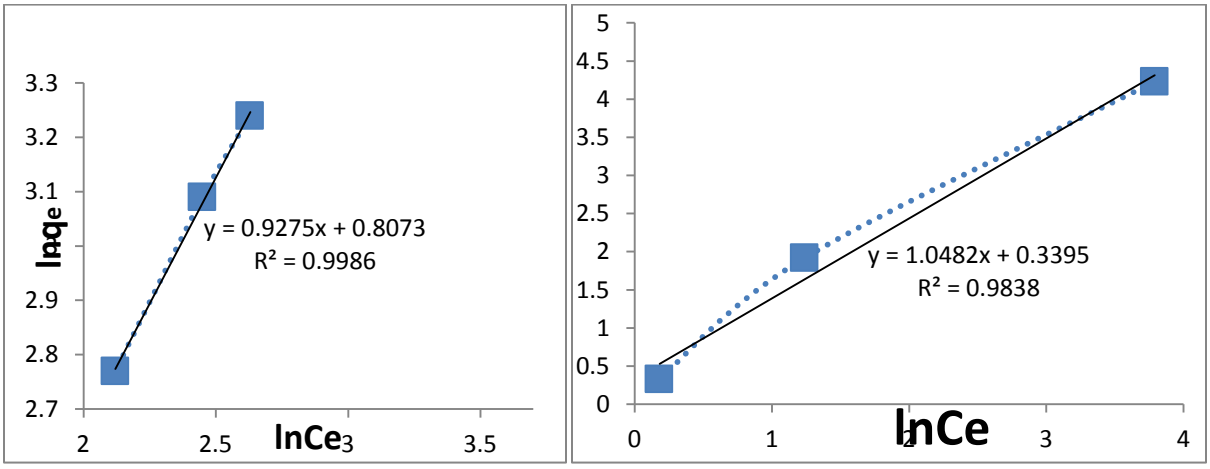

a) b)

Figure 4.17: Freundlich Models for Calcium (a) and Magnesium (b) removal

Table 4.14: Langmuir and Freundlich isotherm parameters of Ca^{2+} and Mg^{2+} adsorption onto synthesized Na-A zeolite from BA

Metal ions	LANGMUIR PARAMETERS				FREUNDLICH PARAMETERS		
	b(L/g)	RL	Qm(mg/g	R^2	KF((mg/g)/(L/mg)1/n)	1/n	R^2
Ca^{2+}	0.0074	0.47	555.54	0.987	2.24	0.9275	0.9986
Mg^{2+}	0.047	0.18	65.78	0.94	1.18	0.93	0.999

4.7.1. Adsorption kinetics

Figure 4.18 a,b and Figure 4.19a,b display the pseudo-first and second order respectively. In the current study, the pseudo first-order and pseudo-second-order models were used for determining the mechanism of the adsorption process. The pseudo-first-order model which assumes that the rate of adsorption site occupation is proportional to the number of unoccupied sites is expressed by the Lagergren equation (Lagergren, 1898) in the linear form as indicated in method section.

The pseudo-second order kinetic model correlation coefficient was R^2 = 1, 0.9643 respectively for Ca^{2+} and $Mg^{2+,}$ suggesting the applicability of the model to the adsorption of Ca2+ and Mg2+ by synthesized zeolite A.

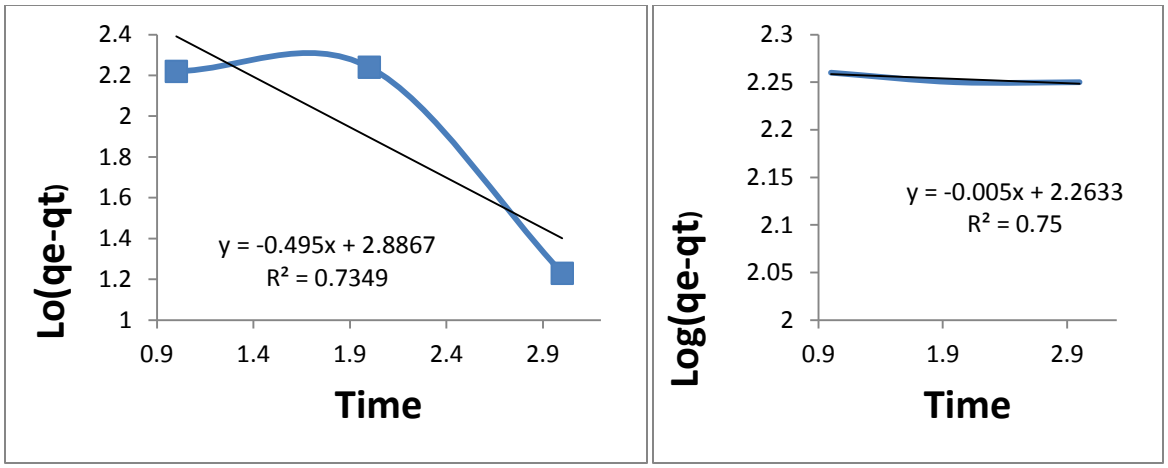

a) b)

Figure 4.18 a,b: Pseudo-first-order model for Ca (a) and Mg (b)

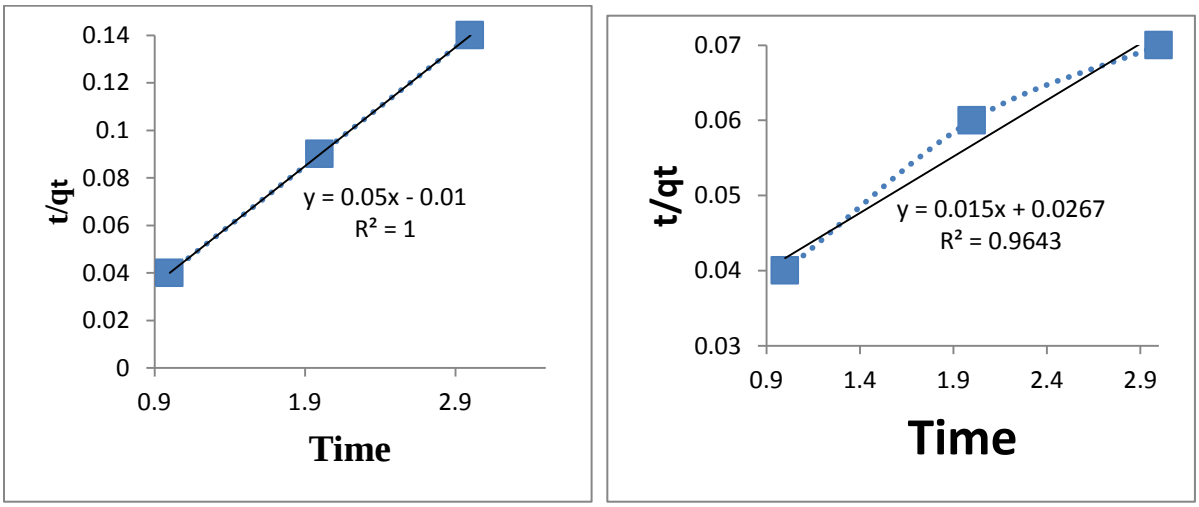

a) Ca b) Mg

Figure 4.19 a,b: Pseudo-second-order kinetic model for Ca (a) and Mg (b)

5. Conclusion and Recommendation

5.1. Conclusion

- This study for the first time confirmed that pure amorphous silica can be successfully extracted from Bagasse Ash. The chemical analysis, XRD and DTG/A data were also indicated the high purity of amorphous silica extracted from Bagasse ash.
- The extracted silica from Bagasse Ash was successfully converted to Na-A zeolite Awith the addition of what XRD analysis result also revealed the formation of pure Na-A zeolite without interference of other crystalline byproduct. In addition, cubic characteristic shape of zeolite A appears on SEM images in conformity with the successful formation of the well-organized zeolitic framework.
- Removal of water hardness by the synthesized Na-A zeolite studied using the batch method indicated factors such as zeolite doses, contact time, initial concentration and pH had significant effect on the removal rate of water hardness causing ions. Moreover, the results indicated that the removal process of ions occurs through ion exchange mechanisms. The maximum sorption capacity of Ca^{2+} was determined to be 555.54ml/g/g and that of Mg^{2+} was 65.78 ml/g/g according to the Langmuir isotherm model. The data reveal the reasonable removal efficiency of ions from water as compared to the previous studies. The kinetic study performed showed the adsorption followed pseudo-second-order kinetic model.
- The overall results obtained showed that Bagasse Ash can be a good source of silica for the synthesis of zeolite A which can be used as an effective cation Exchanger for the removal of Ca^{2+} and Mg^{2+}ions from aqueous solutions.

5.2. Recommendation

Due to time and financial constraints, the scope of this work was limited. Based on the present study, some recommendations can be made for future work. It is first of all recommended that alternative materials such as Filter Cake from Awash Melkassa Aluminium Sulfate, clay and pumice be used in the zeolite synthesis. This will cut down cost considerably as local materials are cheaper than purchasing chemicals.

In this study, ion exchange occurred at room temperature. Increasing the reaction temperatures would enhance the equilibrium point. Working at different temperatures will help to understand the process more as well as note the effect of temperature on the reaction and ion exchange process. The use of alternate methods other than the batch method is highly recommended. Columns or beds could be used to measure the efficiency of zeolites and also produce a water of higher quality.

In addition to water hardness removal the synthesized Na-A zeolite was applied to Deflouridation after surface modification with $FeCl_3$ and 96.4 % removal efficiency was observed. Therefore, to get maximum removing capacity it is important to optimization this work in future and the same thing was done for Chrome removal with high removal capacity, but again the optimization activities was left.

6. References

Abd El Hay, Ali Farrag Th, Abdel Moghny,Atef Mohamed Gad,Saleem Sayed Saleem, Mahmoud Fathy, MuhamedAtef Ahmed. (2016). Removing of Hardness Salts from Groundwater by Thermogenic Synthesis Zeolite**.** sdrp journal of earth sciences and environmental studies.

Barrer, R. M. (1982). Hydrothermal Chemistry of Zeolites. Academic Press, New York.

Barthomeuf, D. (1996). Basic Zeolites: Characterization and Uses in Adsorption and Catalysis. *Catalysis Reviews* **38**(4): 521 – 612.

Breck. D.W.(1974). Zeolites: Molecular Sieves, first ed., Wiley, New York.

Bronić, J., Mužic, A., Antonić Jelić, T., Kontrec, J., and Subotić, B. (2008). Mechanism of crystallization of zeolite A microcrystals from initially clear aluminosilicate solution: A population balance analysis. Journal of Crystal Growth, 310(22), 4656-4665.

Cai, R., Sun, M., Chen, Z., Munoz, R., O'Neill, C., Beving, D. E., and Yan, Y. (2008). Ionothermal Synthesis of Oriented Zeolite AEL Films and Their Application as Corrosion-Resistant Coatings. Angewandte Chemie International Edition, 47(3), 525-528.

Cardoso, N.F., Lima, E.C., Pinto, I.S., Amavisca, C.V., Royer, B., Pinto, R.B., Alencar, W.S., Pereira, S.F.P. (2011). Application of cupuassu shell as biosorbent for the removal of textile dyes from aqueous solution. J. Environ. Manage. (92), 1237–1247.

Denise A. Fungaro, Thais V. S. Reis, Marco Antonio Logli, and Nara A. Oliveira. (2014). "Synthesis and Characterization of Zeolitic Material Derived from Sugarcane Straw Ash." *American Journal of Environmental Protection*, vol. 2, no. 1: 16-21. doi: 10.12691/env-2-1-4.

Dimirkou A and Doula M. K. (2008). "Use of clinoptilolite and an Fe over exchanged clinoptilolite in Zn^{2+} and Mn^{2+} removal from drinking water," *Desalination*, vol. 224, no. 1-3, pp. 280–292.

Dyer, A. and White, K. J. (1999).Cation diffusion in the natural zeolite clinoptilolite.*Chemochimita Acta* **3**: 340 – 348.

EL-Mekkawi, D.M., Ibrahim, F.A., Selim, M.M. (2015). Stability and thermal transformation studies of Zn^{2+} and Fe^{2+}- loaded zeolite.

EL-Mekkawi, D.M., Selim, M.M. (2014). Removal of Pb2+ from water by using Na-Y zeolites prepared from Egyptian kaolins collecte from different sources. J. Environ. Chem. Eng. 2, 723–730. Y prepared from Egyptian kaolin. Solid State Sci. 48, 294–299.

ES (2001). Drinking water specification, 2nd edn. Quality and Standards Authority of Ethiopia, Addis Ababa

Flanigen, E. M. (2001). Molecular Sieve Zeolite Technology- The first Twenty-five Years.Proceedings of the Fifth International Conference on Zeolites, ed. L. V. C. Rees, Heyden London.

Freundlich H. M.(1906). "Over the adsorption in solution," Journal of Phyical Chemisttry, vol. 57, pp. 384–470, 1906.

Gebrekidan M, Samuel Z. (2011).Concentration of heavy metals in drinking water from urban areas of the Tigray Region, Northern Ethiopia. Coll Nat Comput Sci Mekelle Uni 3(1):105–121

Mohamed Ghada M. (2017). Preparation and characterization of Na-A zeolite from aluminum scrub and commercial sodium silicate for the removal of Cd2+ from water. NRC, 33 EL Bohouthst., Dokki-Giza, Egypt.

Gora L., Streletzky K., Thompson R.W., Phillies G.D.J. (1997). Study of the effects of initial-bred nuclei on zeolite NaA crystallization by quasi-elastic light scattering spectroscopy and electron microscopy, Zeolites (19) 98–106.

Gustavo García, Wilson Aguilar, Ivan Carabante, Saúl Cabrera, Jonas Hedlund, Johanne Mouzon (2015). Journal of Alloys and Compounds (619) 771–7

Hadlington S. (2005). Novel ion- exchange technique for zeolites. www.rsc.org/chemistryworld

Hagen, J. (1999). Industrial Catalysis, A Practical Approach. Weinheim, Wiley- VCH.ISBN 3-527-29528-3.

Hoets, J. (2001). Mesoporous Materials.http:// www.chm.bris.ac.uk/webprojects**.**

Hoko Z. (2008). An assessment of quality of water from boreholes in Bindura District, Zimbabwe. Phys Chem Earth 33(8–13):824–828

Htay, M. M., Oo, M. M. (2008). Preparation of Zeolite T catalyst for Petroleum Cracking. World Academy of Science, Engineering and Technology 48, Myanmar.

Hu T, Gao W, Liu X, Zhang Y, Meng C. 2017 Synthesis of zeolites Na-A and Na-X from tablet compressed and calcinated coal fly ash. *R. Soc. open sci.* 4.

Ismail, Adel A R.M. Mohamed, I.A. Ibrahim, G. Kini, B. Koopman. (2010). Synthesis, optimization and characterization of zeolite A and its ion-exchange properties. journal homepage: www.elsevier.com/locate/colsurfa

Kalapathy U., Proctor A., and Shultz J. (2000). "Production and properties of flexible sodium silicate films from rice hull ash silica," *Bioresource Technology*, vol. 72, no. 2, pp. 99–106,

Kulprathipanja, S.(2010).Zeolites in Industrial Separation and Catalysis. Wiley- VCH, Weinham ISBN: 978-3-527-32505-4

Kwakye-Awuah, B. (2008). Production of Silver-loaded zeolites and investigation of their antimicrobial actitvity. Ph.D thesis submitted to the University of Wolverhampton, U.K.

Lagergren S. (1898). "About the theory of so-called adsorption ofsoluble substances," Kungliga Svenska Vetenskapsakademiens Handlingar, vol. 24, pp. 1–39.

Langmuir I. (1918). "The adsorption of gases on plane surfaces of glass, mica and platinum,"The Journal of the American Chemical Society, vol. 40, no. 9, pp. 1361–1403.

Le Blond J. S., Horwell C. J.,. Williamson B. J, and Oppenheimer C. (2010)."Generation of crystalline silica from sugarcane burning," *Journal of EnvironmentalMonitoring*, vol. 12, no. 7, pp. 1459–1470.

Li T, Liu H.,. Fan Y, Yuan P., Shi G., Bi X.T., Bao X.(2012). Synthesis of zeolite Y from natural aluminosilicate minerals for fluid catalytic cracking application, Green Chem. 14. 3255–3259.

Lijalem Ayele, Joaquín Pérez-Pariente,Yonas Chebude, Isabel Diaz.(2015). Synthesis of zeolite A using kaolin from Ethiopia and its application for Detergent. Microporous and Mesoporous Materials journal homepage: www.elsevier.com/locate/micromeso 29-36.

Loiola A.R, Andrade J.C.R.A, Sasaki J.M, da Silva L.R.D. (2017). Structural analysis of zeolite Na-A synthesized by a cost-effective hydrothermal method using kaolin and its use as water softener Journal of Colloid and Interface Science (367)) 34–39.

Manio, S. J. (2000). "Method for Reducing Metal Ion Concentration in Brine Solution," US Patent 6,103,092.

Mirfendereski M. and Mohammadi T. (2011). "Investigation of Hydrothermal Synthesis Parameters on Characteristics of T type Zeolite Crystal Structure," *Journal of Powder Technology*, vol. 206, pp. 345-352.

Mojtaba Mirfendereski1, Toraj Mohammadi . (2016).Effects of Synthesis Parameters on the Characteristics of Naa Type Zeolite Nanoparticles. Paper No. ICNNFC 113 DOI: 10.11159/icnnfc16.113.

Nadir, H. T. (2006).Synthesis and Characterization of Zeolite Beta, MSc Thesis, METU, Ankar of chemistry (40) 3440-3446.

Ohrman, O. (2000). Synthesis and Characterization of Zeolite Coatings on Monoliths Support, MSc Thesis, Lulea University of Technology.

Parnham, E. R., and Morris, R. E. (2007). Ionothermal synthesis of zeolites, metal–organic frameworks, and inorganic–organic hybrids. Accounts of chemical research, 40(10), 1005-1013.

Patcharin Worathanakul, Wisaroot Payubnop, and Akhapon Muangpet. (2009).Characterization for Post-treatment Effect of Bagasse Ash for Silica Extraction. World Academy of Science, Engineering and Technology 56.

Peric J., Trgo M., Medvidovi N.V. (2004). Removal of zinc, copper and lead bynatural zeolite a comparison of adsorption isotherms, Water Research 38, 2004, 1893–1899.

Physics (132), 973-976.

Robson, H. (2001). Verified synthesis of Zeolitic Materials, 2nd Revised Edition, Elsevier Science, Amsterdam.

Saleh. M. M. (2009). "Water softening using packed bed of polypyrrole from flowing solutions," *Desalination*, vol. 235, no. 1–3, pp. 319–329.

Sales A. and Lima S. A. (2010). "Use of Brazilian sugarcane bagasse ash in concrete as sand replacement," *Waste Management*, vol. 30, no. 6, pp. 1114–1122.

Santasnachok, C., Kurniawan, W., Hinode, H. (2015). The use of synthesized zeolites from power plant rice husk ash obtained from Thailand as adsorbent for cadmium contamination removal from zinc mining. J. Environ. Chem. Eng. 3, 2115–2126.

Sapawe N, Jalil AA, Triwahyono S, Shah MIA, Jusoh R, Salleh NFM, Hameed BH, Karim AH. (2013). Cost-effective microwave rapid synthesis of zeolite NaA for removal of methylene blue. *Chem. Eng. J.* (229), 388–398.

Schuring, D. (2002). Diffusion in Zeolites: Towards a Microscopic Understanding. , MSc Thesis, Eindhoven University of Technology

Seifi L., Torabian A., Kazemian H et al. (2011). "Adsorption of BTEX on surfactant modified granulated natural zeolite nanoparticles: parameters optimizing by applying taguchi experimental design method," Clean - Soil, Air, Water, vol. 39, no. 10, pp. 939–948.

Slangen, P. M., Jansen, J. C., and Van Bekkum, H. (1997). The effect of ageing on the microwave synthesis of zeolite NaA. Microporous materials, 9(5), 259-265.

Sobolev, V. I., Panov, G. I. Kharitonov, A. S. Romanikov, V. N., Volodin, A. M. and Ione, K. G. (1993). Catalytic properties of ZSM-5 zeolites in N2O decomposition: the role of iron. *Journal of Catalysis* **139**(2): 435 – 443.

Strathmann, H., Giorno, L., and Drioli, E. (2011). Introduction to membrane science and technology. Wiley-VCH Verlag and Company.

synthesis of pure-form zeolite A from fly ash using two-stage method, J.

Szostak, R. (1992). Handbook of Molecular Sieves, New York, Van Nostrand Reinhold: New York

Thuadaij Pattaranun and Mukda Prasith. (2016).Synthesis and characterization of zeolite derived from Buriram sugarcane bagasse ash and Narathiwat kaolinite**.** SNRU Journal of Science and Technology 8 (3).320–326.

Top, A. (2001). Cation exchange (Ag2+, Zn2+, Cu2+) Behaviour of natural Zeolites,.MSc Thesis, Izmir Institute of Technology, Turkey.

Treacy M.J and Higgins, J.B. (2001). Collection of simulated XRD powder patterns for zeolites, fourth ed., Elsevier, Amsterdam, The Netherlands, 379.

Trif, E., Strugaru, D., Russu, R., Gheorge, G., Nicula, A. (1993). Thermal properties of Y-type zeolites.*Journal of Thermal Analysis and Calorimetry*, **41** (4): 871-880

Tubana B. T and Heckman J. R. (2015). "Silicon in soils and plants," in Silicon and Plant Diseases, F. A. Rodrigues and L. E. Datnoff, Eds., chapter 2, pp. 7–51, Springer International Publishing, Switzerland, Europe.

Upenyu Guyo, Lycenter Yard Phiri, and Fidelis Chigondo. (2017). Application of Central Composite Design in the Adsorption of Ca(II) on Metakaolin Zeolite. Hindawi Journal of Chemistry Volume 2017, Article ID 7025073.

Von Gunten U. (2003). Ozonation of drinking water: part I. Disinfection and byproduct formation in presence of bromide, iodide or chlorine Water Res. Issue 37:1469–1487.

Win, P. (2004).Preparation of Synthetic Zeolitesfrom Myanmar Clay Mineral.Technical Report.CeramicResearch Department.Myanmar Scientific and Technological Research Department. Myanmar..

Xue Z, Li Z, Ma J. et al. (2014). "Effective removal of Mg^{2+} and Ca^{2+} ions by mesoporous LTA zeolite," Desalination, vol. 341, no. 1, pp. 10–18.

Zeolite A using kaolin from Ethiopia and its application for detergents. New Journal

Zhang X., Tang D., and Jiang G. (2013). "Synthesis of zeolite NaA at room temperature: The effect of synthesis parameters on crystal size and its size distribution," *Advanced Powder Technology*, vol. 24, no. 3, pp. 689-696.

Zoller U., P. Sosis. (2008). Handbook of Detergents: Part F, in: Handbook of Detergents, CRC Press.

7. Appendixes

Table 1: Effect of pH on removal of $Ca^{2+}$and Mg^{2+} ions on Na-A zeolite from BA

S.No	Initial pH	Final conc (ppm)		% removal of ions	
		Ca^{2+}	Mg^{2+}	Ca^{2+}	Mg^{2+}
1	6	13.76	19.88	93.12	90.06
2	7	11.61	44	94.20	78.00
3	9	10.43	5.72	94.47	97.14

Table **2**: Effect of contact time on removal of $Ca^{2+}$and Mg^{2+} ions onto Na-A zeolite from BA

S.No	Contact time, (h)	Final conc. (ppm)		% removal o ions	
		Ca^{2+}	Mg^{2+}	Ca^{2+}	Mg^{2+}
1	1	8.90	18.65	95.55	90.67
2	2	11.61	44	96.20	78.00
3	3	8.94	1.63	95.53	99.18

Table 3: Effect of adsorbent dosage on removal of $Ca^{2+}$and Mg^{2+} ions onto Na-A zeolite from BA

S.No	Na-A zeolite dosage, M, (g/L)	Final concn (ppm)		% removal of ions	
		Ca^{2+}	Mg^{2+}	Ca^{2+}	Mg^{2+}
1	0.5	11.61	44	94.20	78.0
2	1	9.84	5.54	95.08	97.23
3	1.5	7.13	1.12	96.43	99.44

Table 4: Effect of initial concentration on removal of $Ca^{2+}$and Mg^{2+} ions onto Na-A zeolite from BA

S.No	Initial concentration, C_o, (ppm)	Final concentration (ppm)		% removal of ions	
		Ca^{2+}	Mg^{2+}	Ca^{2+}	Mg^{2+}
1	100	13.79	1.20	93.10	99.40
2	150	8.35	3.47	95.83	98.26
3	200	11.61	44	95.20	78.0

Table 5: the Langmuir and the Freundlich isotherm data

Final concentration C_e		**adsorption** capacity q_e		**Langmiur** isotherms Ce/qe		**Freundlich** isotherms lnC_e			lnq_e
Ca^{2+}	Mg^{2+}	Ca^{2+}	Mg^{2+}	Ca^{2+}	Mg^{2+}	Ca^{2+}	Mg^{2+}	Ca^{2+}	Mg^{2+}
13.79	1.20	25.68	1.39	0.54	0.86	2.63	0.18	3.24	0.33
8.35	3.47	16.00	6.82	0.52	0.51	2.12	1.24	2.77	1.92
11.61	44	22.11	68.64	0.53	1.99	2.45	3.79	3.09	4.23

Table 6: the value of R_L for each initial concentration of the solution

C_0		R_L	
Ca^{2+}	Mg^{2+}	Ca^{2+}	Mg^{2}
1oo	100	0.12	0.18
150	150	0.47	0.12
200	200	0.4	0.09

Table 7: Langmuir and Freundlich isotherm parameters of Ca2+ and Mg2+adsorption onto synthesized Na-A zeolite from BA

Metal ions	**LANGMUIR PARAMETERS**				**FREUNDLICH PARAMETERS**		
	b(L/g)	RL	qm(me/g)	R^2	$K_F((mg/g)/(L/mg)^{1/n})$	1/n	R^2
Ca^{2+}	0.0074	0.47	555.54.	0.987	2.24	0.9275	0.9986
Mg^{2+}	0.047	0.18	65.78	0.94	1.18	0.93	0.999

Table 8: Pseudo-first order kinetic data for the adsorption of lead ion onto zeolite Na-X

time	$log(q_e-q_t)$	q_e	q_t

	Ca2+	Mg2+	Ca2+	Mg2+	Ca2+	Mg2+
1	2.12	1.95	191.1	198.4	19.11	18.14
2	2.10	1.92	191.1	198.4	18.84	15.6
3	2.00	1.90	191.1	198.4	19.10	19.84

Table 9: Pseudo-second order kinetic data for the adsorption of lead ion onto zeolite Na-X

time	t/q_t		q_t	
	Ca2+	Mg2+	Ca2+	Mg2+
1	0.11	0.10	8.621	9.88
2	0.14	0.14	14.165	14.653
3	0.16	0.19	18.839	15.68